IMMUNOSUPPRESSION-INDEPENDENT ROLE OF REGULATORY T CELLS AGAINST HYPERTENSION-DRIVEN RENAL DYSFUNCTIONS

by

Salvatore Fabbiano[1,2], Mauricio Menacho-Márquez[1,2], Javier Robles-Valero[1,2], Miguel Pericacho[3], Adela Matesanz-Marín[4], Carmen García-Macías[1,2], María A. Sevilla[3], M. J. Montero[3], Balbino Alarcón[5], José M. López-Novoa[3], Pilar Martín[4] and Xosé R. Bustelo[1,2,*]

[1]Centro de Investigación del Cáncer and [2]Instituto de Biología Molecular y Celular del Cáncer, Consejo Superior de Investigaciones Científicas (CSIC)-University of Salamanca, 37007 Salamanca, Spain. [3]Departamento de Fisiología y Farmacología, University of Salamanca, 37007 Salamanca, Spain. [4]Centro Nacional de Investigaciones Cardiovasculares (CNIC), 28029 Madrid, Spain. [5]Centro de Biología Molecular Severo Ochoa, CSIC, 28049 Madrid, Spain.

Running title: A new T_{REG}/neutrophil axis in cardiorenal fibrosis

Key words: Hypertension; heart remodeling; cardiorenal fibrosis; immune system; T_{REG} cells; neutrophils; CD39

Character count (including spaces): 82,728

*To whom correspondence should be addressed (e-mail: xbustelo@usal.es)

ABSTRACT

Hypertension-associated cardiorenal diseases represent one of the heaviest burdens for current health systems. In addition to hemodynamic damage, recent results have revealed that hematopoietic cells contribute to the development of these diseases by generating proinflammatory and profibrotic environments in heart and kidney. However, the cell subtypes involved remain poorly characterized. Here, we report that CD39^{+} regulatory T (T_{REG}) cells utilize an immunosuppression-independent mechanism to counteract renal and possibly cardiac damage during angiotensin II (AngII)-dependent hypertension. This mechanism relies on the direct apoptosis of tissue-resident neutrophils by the ecto-adenosine triphosphate diphosphohydrolase activity of CD39. Consistent with this, experimental and genetic alterations in T_{REG}/T_H cell ratios have a direct impact on tissue-resident neutrophil numbers, cardiomyocyte hypertrophy, cardiorenal fibrosis and, to a lesser extent, in arterial pressure elevation during AngII-driven hypertension. These results indicate that T_{REG} cells constitute a first protective barrier against hypertension-driven tissue fibrosis and, in addition, suggest new therapeutic avenues to prevent hypertension-linked cardiorenal diseases.

INTRODUCTION

Foxp3$^+$CD4$^+$ T_{REG} cells are primarily involved in the negative control of conventional T cell-dependent immune processes. To this end, they utilize a number of effector mechanisms including cytokine-dependent paracrine signaling events, interleukin 2 consumption, presentation of immunosuppressive ligands, cytolysis of target cells, and the modification of cell responses through the degradation of extracellular ATP. This latter regulatory mechanism is mediated by CD39, an ectoenzyme that displays adenosine triphosphate diphosphohydrolase activity (1, 2). In addition, they can promote immunomodulation through the regulation of other hematopoietic cells such as B lymphocytes, dendritic cells, and macrophages (1, 2). Recent observations have revealed that tissue-specific T_{REG} subtypes can also exert immunosuppression-independent functions. The best-characterized examples are T_{REG} cells present in adipose tissue and injured skeletal muscles that control metabolic indexes and muscle repair, respectively. These T_{REG} subsets are distinct from those involved in immunosuppression according to T cell receptor repertoire and transcriptomal features (3, 4).

Hypertension and associated cardiovascular diseases represent nowadays one of the heaviest burdens for our health systems (5, 6). In addition to the hemodynamic-related damage inflicted by hypertension itself, a number of pathophysiological circuits that change the inflammatory, fibrotic, and functional status of peripheral tissues also influence the progression of these dysfunctions. If untreated, these processes eventually lead to end organ disease and failure (7, 8). Extensive data indicates that T_{REG} cells play protective roles against high arterial pressure, cardiovascular remodeling, and heart damage (9-11). The

exact nature of such protective action is unknown, although it has been commonly assumed that it was primarily associated with immunosuppression-linked mechanisms. Consistent with this, a large number of studies have shown that conventional T lymphocytes, the main cellular targets of T_{REG} cells, do play proactive roles during both the initiation and progression of hypertension-related pathophysiological events (8, 12-22). The exact T cell subpopulation(s) involved in those processes is still under debate. Thus, some studies have proposed the implication of different helper T (T_H17, T_H1, T_H2) subtypes in the engagement of these pathophysiological responses (13, 16, 17). By contrast, other analyses have postulated the control of the extent of the hypertensive response is under the regulation of nonconventional $CD3^+CD4^-CD8^-$ T cell subpopulation that are specifically localized in perivascular adipose tissue (15). It is possible that these divergent results could reflect the implication of different T cell subsets in tissue specific pathophysiological responses of the vasculature, heart, and kidney. Settling this issue is of paramount importance to design new approaches to combat the inflammatory processes priming cardiorenal fibrosis and, eventually, end organ disease. In the same context, it is important to clarify the specific role of T_{REG} cells in the regulation of this complex pathophysiological program and the cellular targets that are controlled by them.

The Vav family is a group of phosphorylation-dependent GDP/GTP exchange factors involved in the activation step of Rho proteins. This family has three members in mammalian species that have been designated as Vav1 (formerly known as Vav or $p95^{vav}$), Vav2, and Vav3. Vav1 is primarily expressed in most hematopoietic lineages whereas Vav2 and Vav3 show more widespread expression patterns (23-25). Vav1 and, to a lesser

extent the other family members are important for lymphocyte development, selection, and effector functions (23-25). Consistent with this, single *Vav1*$^{-/-}$ and triple *Vav1*$^{-/-}$;*Vav2*$^{-/-}$;*Vav3*$^{-/-}$ knockout mice exhibit both peripheral T cell lymphopenia and deficient, T cell receptor-dependent antigenic responses (26-28). Vav2 and Vav3, but not Vav1, are also involved in signaling routes contributing to cardiovascular homeostasis. As a consequence, the single and compound elimination of these two proteins causes hypertension, cardiovascular remodeling, cardiorenal fibrosis, and renal dysfunctions in mice (29-32). Based on those observations, we believed that this collection of Vav family knockout mice could represent a useful tool to clarify obscure aspects of the interplay between the immune and cardiovascular systems during hypertension. The use of those animals, together with other experimental mouse models for immunodeficiency and hypertension, allowed us to discover a hitherto unknown T_{REG} cell-dependent mechanism that controls the extent of the overall arterial pressure response and end organ dysfunctions during AngII-dependent hypertension conditions. As we show here, this mechanism is unexpectedly mediated by the direct, CD39- and apoptosis-mediated homeostatic control of tissue-resident neutrophil numbers rather than on standard T cell immunosuppression processes. Hence, it is fully operative even in complete absence of conventional T lymphocytes. This new mechanism offers potentially interesting therapeutic avenues to prevent cardiorenal fibrosis and ensuing end-organ disease in patients with long-term, AngII-dependent types of hypertension.

MATERIALS AND METHODS

Animals. *Vav1*$^{-/-}$ and *Vav2*$^{-/-}$;*Vav3*$^{-/-}$ mice have been previously described (27, 29, 30). All *Vav* family knockout mice were homogenized in the C57BL/10 genetic background. *Ly5.1*$^{+}$ mice were originally obtained from The Jackson Laboratories and maintained at the animal facility of the Centro de Biología Molecular Severo Ochoa (CSIC, Madrid, Spain). For the experiments, animals were transferred to the animal facility of the Centro de Investigación del Cáncer. BALB/c, SCID/Beige (C.B-17/lcrHsd-*Prkdc*^{scid}*Lyst*$^{bg\text{-}J}$), and *Foxn1*^{nu} mice were obtained from Harlan Laboratories. For all *in vivo* studies, animals of the same genotype were randomly assigned to the different experimental groups. Animals used were either four- (in the case of analysis of basal conditions) or three-month (in the case of analyses using osmotic pumps) old. All animal work has been done in accordance with protocols approved by the Bioethics committees of the University of Salamanca, CSIC, and Centro Nacional de Investigaciones Cardiovasculares.

Blood pressure-related analyses. Mean blood pressure was recorded in conscious mice with the non-invasive tail cuff method (CODA, Kent Scientific). Mice were familiarized with the procedure during the week previous to data recording to minimize stress-related blood pressure variations. Blood pressure measurements were always done in the afternoon.

Histological analyses. Tissues were fixed in 4% paraformaldehyde in phosphate-buffered saline solution, paraffin-embedded, cut in 2-3 μm sections and stained with hematoxylin

and eosin (Sigma). Aorta media walls and cardiomyocyte areas were quantified with MetaMorph software (Universal Imaging).

Tissue fibrosis determinations. Fibrosis was quantified both immunohistochemically and biochemically. In the former case, paraffin-embedded tissue sections were stained with Sirius Red (Fluka). In the latter case, we measured the amount of hydroxyproline present in tissue lysates. Data from those analyses were converted into amount of collagen by considering the presence of 12.7% of hydroxyproline residues in that protein. These two procedures were done as indicated before (29, 30).

Analysis of kidney function. Mice were placed in metabolic cages and daily urine production was collected and measured, as indicated before (30). Protein content in urine was detected with Bradford Protein Assay Reagent (Bio-Rad) using a standard curve of bovine serum albumin (Sigma). To calculate creatinine clearance rates, we collected urine from individual mice for a 24 hour-long period using metabolic cages. In addition, we took blood samples from animals under study by cardiac puncture to measure the creatinine concentration in plasma. Urine and plasma creatinine concentrations were determined by a kinetic colorimetric method using a creatinine assay kit (QuantiChrom™ Creatinine Assay Kit, BioAssay Systems) according to the manufacturer's protocol. Creatinine clearance rate (CCR) was calculated taking into account the urine flow (uf) and concentrations of creatinine in both urine ([Cre]u) and plasma ([Cre]p) using the formula $CCR = fu \times [Cre]u / [Cre]p$. Values were further normalized taking into account the weight of kidneys.

149 **Determination of mRNA abundance.** RNA was extracted with TRIzol (Sigma) and
150 quantitative RT-PCR performed with ScriptOne-Step RT-PCR Kit (Bio-Rad) on a
151 StepOnePlus Real-Time PCR System (Applied Biosystems). Data were analyzed with the
152 StepOne software v2.1 (Applied Biosystems). Expression of the endogenous mouse *P36b4*
153 transcript was used as normalization control. Primers used were 5'-TTG ATG ATG GAG
154 TGT GGC ACC-3′ (forward for mouse *P36b4* cDNA), 5'-GTG TTT GAC AAC GGC
155 AGC ATT-3′ (reverse for mouse *P36b4* cDNA), 5'-CAC CAC GGA CTA CAA CCA GTT
156 CGC-3' (forward for mouse *Lcn2* cDNA), and 5'-TCA GTT GTC AAT GCA TTG GTC
157 GGT G-3' (reverse for mouse *Lcn2* cDNA).
158
159 **Pharmacological mouse treatments.** AngII (1.44 mg/kg/day, Sigma) and ARL67156 (1.1
160 μg/kg/day, Sigma) were administered for 14 days using osmotic delivery pumps (Model
161 1002, Alzet) inserted subcutaneously in back of animals. L-NAME (70 mg/100 ml, Sigma)
162 was administered in the drinking water for four weeks (32). MMF (CellCept, Roche Farma)
163 was prepared as previously described (33) and administered as indicated in experiments.
164
165 **Isolation of hematopoietic cells from tissues.** To isolate kidney-infiltrating cells,
166 anesthetized mice were infused phosphate-buffered saline solution through the heart left
167 ventricle to eliminate kidney-resident circulating cells. The two kidneys of each mouse
168 were then collected, decapsulated, cut into small pieces with a sterile scalpel, and incubated
169 in 10 ml of RPMI containing 10% fetal bovine serum and collagenase (5 mg, Sigma) 20
170 min at 37 ºC. After filtering tissue debris, cells were washed twice with phosphate-buffered

171 saline solution and resuspended in 8 ml of Roswell Park Memorial Institute (RPMI) media
172 plus 10% fetal bovine serum. Upon addition of a 5 ml lower layer of Ficoll (Sigma) with a
173 pipette, samples were centrifuged at 2,000 rpm at room temperature for 10 min. Cells in
174 the medium/Ficoll interface were collected using a pipette and counted. To obtain cells
175 from spleen and thymus, single cell suspensions were obtained by mechanical
176 homogenization of tissues in 1 ml of phosphate-buffered saline solution supplemented with
177 2% bovine serum albumin and 0.5 mM EDTA. Bone marrow neutrophils were obtained by
178 flushing the medullar cavity of isolated femoral bones with phosphate-buffered saline
179 solution. In the case of circulating cells, blood samples were collected from hearts with the
180 aid of heparinized syringes. Cell suspensions obtained in the above conditions were washed
181 once in phosphate-buffered saline solution, subjected to 0.17 M NH_4Cl lysis to eliminate
182 erythrocytes, and finally washed twice. Final cell pellets were resuspended in phosphate-
183 buffered saline solution before the immunostaining step.
184
185 **Characterization and isolation of hematopoietic cell percentages.** Cell suspensions
186 obtained as indicated above were stained with combinations of fluorescein isothiochyanate
187 (FICT)-, allophycocyanin (APC)-, APC-Cy7- or V500-labeled antibodies to CD4 (BD
188 Biosciences); FITC-, Pacific blue (PB)- or phycoerythrin (PE)-labeled antibodies to CD8
189 (BD Biosciences); APC- or PE-Cy7-labeled antibodies to CD25 (BD Biosciences); FITC-
190 or APC-labeled antibodies to Gr1 (eBioscience and BD Biosciences, respectively); APC- or
191 PE-Cy7-labeled antibodies to F4/80 (eBioscience and BD Biosciences, respectively); PE-
192 labeled antibodies to CD11b (BD Biosciences); PE- or FITC-labeled antibodies to CD11c

193 (BD Biosciences); biotin- or APC-labeled antibodies to B220 (BD Biosciences) or PE-Cy7
194 labeled anti-CD39 (eBioscience). Cell immunolabeling with either FITC- or PE-labeled
195 antibodies to Foxp3 was done using the Foxp3 Staining Buffer Set (eBioscience). For data
196 acquisition, samples were collected using a FACSAria III flow cytometer (BD Biosciences)
197 and blindly analyzed using the FlowJo software (Tree Star). For in vitro studies, samples
198 were sorted in sterile condition using a FACSAria III system, collected in phosphate-
199 buffered saline solution supplemented with 50% fetal bovine serum, centrifuged,
200 resuspended in RPMI (Gibco Life Technologies) supplemented with 10% fetal bovine
201 serum, 2 mM L-glutamine and antibiotics (100 units/ml Penicillin and 100 μg/ml
202 Streptomycin, Invitrogen) (referred hereafter as complete media), and cultured in complete
203 RPMI media as indicated.
204
205 **iT_{REG} cell generation.** Freshly sorted splenic, $CD4^+CD25^-$ T cells were plated (1×10^6
206 cells/ml) onto culture dishes coated with antibodies to mouse CD3 (5 μg/ml, BD
207 Biosciences) and containing complete RPMI media supplemented with antibodies to CD28
208 (5 μg/ml, BD Biosciences), transforming growth factor β_1 (5 ng/ml, R&D Systems) and
209 recombinant mouse interleukin 2 (100 IU/ml, Peprotech) for four days. Cells were then
210 centrifuged, washed twice with phosphate-buffered saline solution, stained with FITC-
211 labeled anti-CD4 (BD Biosciences), APC-labeled anti-CD25 (BD Biosciences), and PE-
212 Cy7-labeled anti-CD39. The iT_{REG} cell population was separated either as a whole
213 $CD4^+CD25^+$ population or fractionated into $CD4^+CD25^+CD39^+$ and $CD4^+CD25^+CD39^-$

214 populations before being injected into animals. Cells were collected for in vivo experiments
215 using a FACSAria cell sorter as above.
216
217 **T_{REG} injections in mice.** iT_{REG} generated as above and freshly sorted splenic $CD4^+CD25^+$
218 nT_{REG} cells were resuspended in 100 μl of phosphate-buffered saline solution at a cell
219 density of 2×10^6 cells/ml and injected into the lateral tail vein one day after the
220 implantation of the drug delivery pumps. Unless otherwise stated, 2×10^5 cells were
221 injected per animal in these experiments. When indicated, injections were performed with
222 splenic-derived $CD4^+CD25^-$ T cells as above.
223
224 **Immunodepletion of nT_{REG} cells.** 250 μg of either a monoclonal rat antibody to mouse
225 CD25 (clone PC61.5, eBioscience) or an IgG1K isotype negative control (eBioscience)
226 were injected intraperitoneally one day before the implantation of drug delivery osmotic
227 pumps. Extent of immunodepletion achieved in each animal was assessed weekly by flow
228 cytometry. To that end, blood from anesthetized mice was drawn, cells collected, washed in
229 phosphate-buffered saline solution, subjected to 0.17 M NH_4Cl-mediated erythrocyte lysis,
230 washed twice with phosphate-buffered saline solution, stained with both FITC-labeled CD4
231 and APC-labeled CD25, and analyzed by flow cytometry.
232
233 **Immunodepletion of neutrophils.** *WT* mice were intraperitoneally injected with either 500
234 μg of a rat monoclonal antibody to the Ly6G surface marker (clone 1A8, Biolegend) or the
235 same amount of an IgG1K isotype negative control (eBioscience) one day before

implantation of AngII-delivery osmotic pumps. Percentages of neutrophils in blood were assessed every three days by flow cytometry using FITC-labeled antibodies to Gr1. At the end of experiments, percentages of neutrophils, macrophages, and $CD4^+$ T cells in kidneys were determined by labeling cells with antibodies to Gr1 (FITC-labeled, eBiosciences), CD11b (PE-labeled, BD Biosciences), F4/80 (APC-labeled, BD Biosciences), and CD4 (V500-labeled, BD Biosciences).

Neutrophil recruitment assays. When indicated, conditioned cell culture supernatants were obtained from fresh cultures of indicated splenic T cells at 1 x 10^6 cells/ml. After 72 hours, cells were centrifuged and supernatants collected. For chemotactic assays, 1 x 10^5 of freshly purified bone marrow neutrophils were placed onto the upper chamber of a transwell plate (Corning HTS 24 well transwell, 3.0 μm pore size) that contained in the lower chamber complete RPMI, cell-conditioned supernatants from indicated cell types and, when indicated complete RPMI supplemented with 1 μM angiotensin II.

Determination of ROS production and apoptosis in neutrophil cultures. Freshly sorted bone marrow neutrophils were cultured in complete RPMI and treated with 1 μM AngII II for 20 min. When indicated, cells were pretreated with either 10 μM losartan (Merck) or 10 μM PD123319 (Sigma) for 30 min. 10 μM MMF (CellCept, Roche Farma) was included in cultures for 120 min before the angiotensin II stimulation. For neutrophil/nT_{REG} cell coculture experiments, cells sorted as indicated above, treated or untreated with 250 μM ARL67156 in complete RMPI for 30 min, and then cultured together in same culture media

for 24 hours always using 1:10 nT_{REG} cell:neutrophil ratios. In some of these experiments, nT_{REG} cells were either substituted or cocultured with other T cells following the same experimental procedure. Neutrophil ROS production and apoptosis were assessed using lucigenine-based chemiluminescence (34) and annexin V/propidium iodide flow cytometry determinations (35), respectively. The latter assay was done using the Apoptosis Detection kit from Immunostep.

Statistics. Data were analyzed with either a two-tailed Student's *t* test or a one-way ANOVA with Bonferroni post hoc test in the case of multiple comparisons.

RESULTS

Vav proteins are important for hypertension-driven cardiorenal fibrosis

We have reported before that *Vav2*$^{-/-}$, *Vav3*$^{-/-}$, and *Vav2*$^{-/-}$;*Vav3*$^{-/-}$ (*DKO*) knockout mice develop hypertension in an age- and AngII-dependent manner (**Fig. 1A**) (29, 30, 32). Further analyses indicated that *DKO* mice also develop hypertension-linked dysfunctions similar to those present in the single *Vav2*$^{-/-}$ and *Vav3*$^{-/-}$ knockout animals, including the thickening of the aorta media wall (**Fig. 1**, **B** [left panels] and **C**), hypertrophy of left ventricle cardiomyocytes (**Fig. 1, B** [second column from left] and **D**) and interstitial fibrosis in both heart (**Fig. 1**, **B** [third column from left] and **E**) and kidney (**Fig. 1**, **B** [right panels] and **F**). Signs of the latter condition included the detection of collagen with Sirius red staining (**Fig. 1B**, third and fourth panels from left) and hydroxyproline tissue content (**Fig. 1**, **E** and **F**) in both heart and kidney tissue samples. Furthermore, the histological analyses of kidneys revealed the presence of extensive glomerular sclerosis, necrosis of distal tubules, and protein casts in kidney sections from *DKO* mice (**Fig. 1G**). Consistent with this, we observed that *DKO* mice also exhibit alterations in renal physiology such as reduced flow of urine (**Fig. 1H**), increased protein content in urine (proteinuria, **Fig. 1I**), reduced creatinine clearance rates (**Fig. 1J**) and increased amounts of the transcript for lipocalin 2 (Lcn2, **Fig. 1K**), a well-known early biomarker for both acute and chronic nephropathies (36). These results led us to investigate the effect of the additional inactivation of the *Vav1* gene in this cardiovascular phenotype using the triple *Vav1*$^{-/-}$;*Vav2*$^{-/-}$;*Vav3*$^{-/-}$ knockout (*TKO*) mouse strain. We found that these mice exhibit hypertension (**Fig. 1A**) and vascular remodeling (**Fig. 1**, **B** [left panels] and **C**), although at

290 statistically significant lower values than those seen in *DKO* mice (**Fig. 1**, **A** and **C**).
291 However, we unexpectedly found that they show no obvious signs of the cardiomyocyte
292 hypertrophy (**Fig. 1**, **B** [second column from left] and **D**) and cardiorenal fibrosis (**Fig. 1**, **B**
293 [third and fourth columns from left], **E** and **F**). They also show normal rates of urine
294 production (**Fig. 1H**), urine protein content (**Fig. 1I**), creatinine clearance (**Fig. 1J**) and
295 intrarenal amounts of *Lcn2* transcripts (**Fig. 1K**), further indicating that these mice do not
296 have any significant signs of heart remodeling and cardiorenal fibrosis in the kidneys.

297 We surmised that the mild hypertension present in *TKO* mice could be the cause of
298 the protection exhibited by these animals against cardiorenal fibrosis and cardiovascular
299 remodeling. To explore this possibility, we decided to compare the foregoing
300 pathophysiological parameters in wild-type (*WT*), *DKO* and *TKO* mice under systemic
301 administration conditions of AngII, a well-known vasoconstriction agent (37). We
302 speculated that if the above idea were correct, then the chronic delivery of this
303 vasoconstriction agent had to restore cardiorenal fibrosis and heart remodeling in *TKO*
304 mice. To this end, we implanted AngII-delivery osmotic pumps on the backs of *WT*, *DKO*
305 and *TKO* animals and, subsequently, followed the evolution of blood pressure during a 14
306 day-long period. In addition, we monitored the rest of cardiovascular and renal parameters
307 using samples from mice euthanized at the end of AngII treatment. As expected, such
308 conditions promote the development of high blood pressure (**Fig. 1L**), renal fibrosis (**Fig.**
309 **1M**), and increased amounts of *Lcn2* transcripts in kidneys (**Fig. 1N**) in *WT* mice.
310 Likewise, they exacerbate the hypertensive state of *DKO* mice (**Fig. 1L**). However, this
311 change in arterial blood pressure does not lead to further increases in the already high levels

312 of collagen deposition (**Fig. 1M**) and *Lcn2* mRNA expression (**Fig. 1N**) present in the
313 kidneys of these mice. The systemic infusion of AngII also aggravates the hypertension
314 state of *TKO* mice, although to a lower extent to those found in AngII-infused *DKO* and
315 *WT* mice (**Fig. 1L**). However, arterial blood pressure does reaches under those conditions
316 levels comparable to those exhibited by the untreated *DKO* mice (**Fig. 1L**) that, as shown
317 above, do develop cardiorenal fibrosis (**Fig. 1**, **C** to **K**). Despite this, the AngII-treated *TKO*
318 mice still do not show any change in renal fibrosis-related parameters (**Fig. 1**, **M** and **N**).
319 These results suggest that the differences in overall arterial blood pressures could not be the
320 main leading cause of the different cardiorenal phenotypes exhibited by *DKO* and *TKO*
321 mice. In addition, they indicate that Vav proteins play either direct or indirect roles in
322 hypertension-driven cardiorenal fibrosis.
323
324 **The *Vav1* gene deficiency is sufficient to confer protection against tissue fibrosis**
325 To investigate whether the protection exhibited by *TKO* mice against heart remodeling and
326 cardiorenal fibrosis was due to the elimination of the three *Vav* family genes or to the single
327 inactivation of the *Vav1* gene, we next compared the response of control and single $Vav1^{-/-}$
328 knockout mice to the systemic administration of AngII. With the exception of the normal
329 development of vascular remodeling (**Fig. 2A**), AngII-infused $Vav1^{-/-}$ mice develop no
330 obvious signs of cardiomyocyte hypertrophy (**Fig. 2B**), cardiorenal fibrosis (**Fig. 2**, **C** and
331 **D**) or changes in the expression of the *Lcn2* mRNA in kidneys (**Fig. 2E**). Furthermore,
332 although AngII-infused $Vav1^{-/-}$ mice initially show elevations in blood pressure similar to
333 controls (**Fig. 2F**), they eventually undergo smaller hypertensive responses than *WT*

334 animals at later periods of the systemic administration of AngII (**Fig. 2**, **F** and **G**). The time
335 of the differential response takes place between the 6th and the 10th day of AngII infusion,
336 which roughly corresponds to the time in which the cardiorenal fibrosis reaches a plateau in
337 control mice (**Fig. 2H**). Thus, the elimination of the Vav1 gene fully recapitulates the
338 effects derived from the removal of the three Vav family members in this
339 pathophysiological scenario. Unlike the case of AngII-driven hypertension, we observed
340 that the *Vav1*$^{-/-}$ mice are not protected against the dysfunctions under study when treated
341 with the nitric oxide synthase inhibitor Lω-Nitro-L-arginine methyl ester (L-NAME) (**Fig.**
342 **2**, **I** to **N**). This compound promotes hypertension through the blockage of the nitric oxide-
343 mediated dilatation of resistance blood vessels (38). These results suggest that the
344 antifibrotic protection induced by the *Vav1* gene deficiency is not probably due to a
345 nonspecific, buffering effect on the damaging hemodynamic effects of hypertension on
346 peripheral tissues.
347
348 **Immunosuppressed mice show no resistance to hypertension-linked tissue fibrosis**
349 *Vav1*$^{-/-}$ and *TKO* mice, unlike the case of *DKO* animals, have reduced numbers of
350 peripheral T cells that, in addition, cannot adequately respond to antigens (26-28). Based on
351 previous reports indicating that conventional T cells are implicated in the development of
352 hypertension, tissue fibrosis and end-organ disease (7, 8, 12, 13, 20), we surmised that the
353 lymphopenic status of those two mouse strains could be the main cause of the resistance
354 shown to AngII-triggered heart remodeling and cardiorenal fibrosis. If that were the case,
355 we assumed that a similar phenotype had to be found in other immunocompromised mice.

In agreement with both this idea and published results (12, 13), we initially found that the treatment of AngII-infused *WT* mice with the T cell immunosuppressant mycophenolate mofetil (MMF)(39) does lead to a hypertensive buffering effect and protection against cardiorenal fibrosis (SF, data not shown). As an additional control to corroborate these results, we next decided to analyze the response of *Foxn1*^{nu} mice, a strain that cannot generate T lymphocytes due to problems in the development of the thymus, to the infusion of AngII. Unexpectedly, we found in this case no significant protection against the cardiorenal fibrosis (**Fig. 3**, **A** and **B**) and a total lack of the hypertension buffering effect (**Fig. 3**C) that had been previously seen in *Vav1*$^{-/-}$ mice. Similar results were obtained with AngII-treated severe combine immunodeficiency (SCID)/Beige mice that lack both T and B lymphocytes (SF, data not shown, see also **Fig. 7** below). We inferred from these experiments that T cell immunosuppression per se cannot explain the results obtained with *Vav1*$^{-/-}$ and MMF-treated *WT* mice and, therefore, that other cell types had to be involved in the development of cardiorenal fibrosis during AngII-triggered hypertension. Concurring with this idea, we found that MMF also promotes resistance to both cardiorenal fibrosis (**Fig. 3**, **A** and **B**) and excessive elevations of blood pressure (**Fig. 3C**) when administered to AngII-infused *Foxn1*^{nu} mice.

Taking into account that the *Vav1* gene is predominantly expressed in hematopoietic cells (23), we hypothesized that alterations in cells belonging to either the adaptative or innate immune had to be involved in the protection against fibrosis exhibited by *Vav1*$^{-/-}$ mice. As a first approximation to identify them, we next carried out flow cytometry determinations to analyze the distribution of a large variety of hematopoietic cell lineages

in the kidneys, blood, spleens, and thymi from *DKO* (which showed no cardiorenal protection), *TKO* (which exhibited cardiorenal protection), *Vav1*$^{-/-}$ (normotense and immunodeficient), and normotense *WT* mice. We excluded the heart from these studies due to the difficulty in avoiding crosscontamination from the large numbers of circulating cells present in that tissue. We found that *TKO* and *Vav1*$^{-/-}$ mice have reduced numbers of both neutrophils and CD4^{+} cells in kidneys when compared to the other mouse strains (**Table 1**). This neutropenia is kidney-specific, because no statistically significant differences are detected in circulating neutrophils between *TKO* and *DKO* mice (**Table 1**). However, these two mouse knockout strains do exhibit neutrophilia in the blood when compared to *WT* and *Vav1*$^{-/-}$ animals (**Table 1**). Whether this is due to their common hypertensive condition remains unknown. Unlike the case of neutrophils, the CD4^{+} T cell lymphopenia found in kidneys of *TKO* and *Vav1*$^{-/-}$ mice is also seen in the rest of tissues surveyed (**Table 1**), a result consistent with the known intrathymic T cell selection defects present in those mice (27). Unexpectedly, further flow cytometry analyses revealed that the CD4^{+} T cell lymphopenia of *TKO* and *Vav1*$^{-/-}$ mice does not apply to CD4^{+}Foxp3^{+} T_{REG} cells, because the percentage of these immunoregulatory cells is comparable to those present in *WT* and *DKO* animals in all tissues surveyed (**Table 1**). By contrast, we observed no statistically significant variations in the percentages of other hematopoietic lineages surveyed, including macrophages, CD11c^{+} and CD11c^{-} dendritic cells, CD8^{+} T cells, and B lymphocytes in kidneys of control, *DKO*, *TKO,* and *Vav1*$^{-/-}$ mice (**Table 1**). These results suggested that T_{REG} cells, neutrophils or both cell lineages combined could be potentially

399 involved in the protection against cardiorenal protection seen in *TKO*, AngII-infused *TKO*,
400 and AngII-infused *Vav1*$^{-/-}$ mice.
401
402 **T_{REG} cells promote protection against hypertension-driven cardiorenal fibrosis**
403 Owing to the above results, we decided to investigate the possible implication of T_{REG} cells
404 in the protection against hypertension-driven cardiorenal fibrosis shown by *Vav1*$^{-/-}$ mice.
405 As a first approximation, we decided to analyze whether the artificial increase in the
406 T_{REG}/T_H ratio in *WT* mice could reproduce the protection offered by the *Vav1* gene
407 deficiency against cardiorenal fibrosis. To this end, we generated in vitro T_{REG} cells
408 (referred hereafter as iT_{REG}) by culturing splenic *WT* $CD4^+CD25^-$ lymphocytes in the
409 presence of a differentiation cocktail and, upon purification by flow cytomery (**Fig. 4A**,
410 second and third panels from left), injected them into recipient *WT* mice. We carried out
411 two independent control experiments to make sure that this approach led to effective
412 changes in the T_{REG}/T_H cell ratio in the recipient mice. Firstly, we confirmed by flow
413 cytometry that we were actually injecting T_{REG} cells, since ≈80% of the cells differentiated
414 in vitro were positive for the T_{REG} cell-specific Foxp3 transcriptional factor (**Fig. 4A**, right
415 panel). Secondly, by using pilot injection experiments of iT_{REG} cells generated from
416 C57BL/6 Ly5.1 mice (whose hematopoietic cells are $CD45.1^+$) into *WT* C57BL/10 mice
417 (whose hematopoietic cells are $CD45.2^+$), we could estimate that the chosen experimental
418 protocol does promote a three- and two-fold increase in the total amount of T_{REG} cells in the
419 recipient mice during the first six and late postinjection days, respectively (**Fig. 4B**, see plot
420 with closed boxes). These variations are directly derived from the iT_{REG} cells ($CD45.1^+$) that

had been injected into mice (**Fig. 4B**, see plot with open boxes). Moreover, we found that the injected iT_{REG} population maintains the $CD4^+CD25^+$ status during an extended period of time, although it undergoes a two-fold decrease at the latest time point analyzed (**Fig. 4C**, see lanes with light blue boxes). As a result, we calculated that the injected animals maintain high T_{REG}/nonT_{REG} $CD4^+$ cell ratios during most of the time course used in these studies (**Fig. 4C**, compare lanes with light blue and light red boxes). When we repeated these injection experiments with standard CD57BL/10 iT_{REG} cells, we observed that the recipient *WT* mice exhibit no cardiorenal fibrosis (**Fig. 4**, **D** and **E**) and a buffered hypertensive response (**Fig. 4F**) upon the systemic administration of AngII. Based on the results obtained in the analyses of hematopoietic cells present in Vav family knockout mice (**Table 1**), we also decided to include as an additional read-out in these studies the evolution of neutrophil numbers present in the kidneys of iT_{REG}-injected mice. We observed that these mice show a significant reduction in the percentage of neutrophils in the kidneys when compared to controls (**Fig. 4**, **G** and **H)**, thus suggesting a possible direct link between the elevated T_{REG}/T_H ratios and the kidney neutropenia previously inferred from the experiments with *TKO* mice (see above, **Table 1**). Interestingly, this latter effect is also observed in mice not treated with AngII (**Fig. 4I**), possibly indicating a hypertension-independent crosstalk between T_{REG} cells and neutrophils in this tissue. Using a similar experimental approach, we demonstrated that the expression of Vav1 is not important for the efficient generation (**Fig. 4J**) and functionality (**Fig. 4K**) of iT_{REG} cells in this experimental setting. Thus, it is unlikely that the phenotype observed in *Vav1*$^{-/-}$ mice could be directly caused by the presence of nonfunctional T_{REG} cells in kidneys.

443 To further confirm the implication of T_{REG} cells in this process, we next assessed the
444 effect of eliminating T_{REG} cells in *Vav1*$^{-/-}$ mice. According to our hypothesis, such a
445 procedure had to restore fibrosis in the kidneys of these animals and induce a concomitant
446 increase in the number of intrarenal neutrophils. To achieve this end, we carried out an
447 immunodepletion strategy consisting in injecting the animals under study with an antibody
448 to the high affinity interleukin 2 receptor (CD25). As shown in **Fig. 5A**, this procedure
449 promotes the efficient and long-term elimination of T_{REG} cells in mice. When infused with
450 AngII, we observed that T_{REG}-immunodepleted *Vav1*$^{-/-}$ mice behave like *WT* mice in terms
451 of cardiorenal fibrosis development (**Fig. 5**, **B** and **C**) and elevation in blood pressure (**Fig.**
452 **5D**). Importantly, we found that these mice also recover *WT*-like percentages of kidney-
453 resident neutrophils both under AngII administration (**Fig. 5**, **E** and **F**) and basal (**Fig. 5G**)
454 conditions. In addition to further confirm the negative crosstalk between T_{REG} and
455 neutrophils, these results suggest that the intrakidney neutropenia previously detected in
456 both AngII-treated and untreated *Vav1*$^{-/-}$ mice (see above, **Table 1** and **Fig. 4**) cannot be
457 caused by intrinsic signaling dysfunctions of the *Vav1*$^{-/-}$ neutrophils. Collectively, these
458 findings support the idea of a direct functional link between T_{REG}/T_H ratios and neutrophil
459 numbers that, eventually, modulate AngII-driven tissue fibrosis in hypertensive mice.
460
461 **Neutrophils contribute to hypertension-driven cardiorenal fibrosis**
462 Given the direct correlation between effective fibrosis development and neutrophil numbers
463 observed in the foregoing experiments, we next decided to address the direct contribution
464 of these myeloid cells to this process. To this end, we immunodepleted them in *WT* mice

using injections with an antibody (1A8) to the Ly6G subunit of the Gr1 antigen. The efficient depletion of these cells was confirmed by detecting the percentage of $Gr1^+$ cells in the blood of injected animals using flow cytometry analyses (**Fig. 6A**). Using this approach, we observed that neutrophil-depleted *WT* mice phenocopy the *Vav1* gene deficiency in terms of protection against cardiorenal fibrosis (**Fig. 6**, **B** and **C**) and development of mild hypertensive responses (**Fig. 6D**) when systemically infused with AngII. This effect is neutrophil-dependent, because the kidneys of the mice pretreated with the 1A8 antibody exhibit percentages of macrophage (**Fig. 6E**) and $CD4^+$ T cells (**Fig. 6F**) similar to those found in control mice. However, under the same conditions, they show the expected lack of neutrophils in this organ (**Fig. 6, G** and **H**). These results indicate that neutrophils are critical for the induction of all those AngII-triggered pathophysiological responses even in fully immunocompetent mice.

T_{REG} cells protect against hypertension-driven fibrosis in immunodeficient mice

To further rule out that the antifibrotic effect of iT_{REG} cells was independent on their roles in general T cell immunosuppression, we decided to repeat some of the above experiments in AngII-infused SCID/Beige (C.B-17/lcrHsd-*Prkdc*^{scid}*Lyst*$^{bg\text{-}J}$) and *Foxn1*^{nu} mice. SCID/Beige mice are totally devoid of T and B lymphocytes due to a SCID mutation that impairs the V(D)J recombination of antigen receptor genes in these two cell lineages. They also have diminished natural killer cell and macrophage activity owing to the presence of the beige mutation. As controls for these animals, we used immunocompetent mice of the same genetic background (BALB/c). Similarly to our results with *WT* C57BL/10 animals (see

487 above, **Fig. 4**), we observed that the injection of iT_{REG} cells promotes protection against
488 AngII-induced renal fibrosis in SCID/Beige mice (**Fig. 7**, **A** to **C**), BALB/c (**Fig. 7**, **A** to
489 **C**), and *Foxn1*^{nu} mice (**Fig. 7**, **D** and **E**; red bars). These effects are associated with parallel
490 reductions in the normal percentages of neutrophils present in the kidneys of those animals
491 (**Fig. 7, F** to **H**). As negative control, we did not observe any significant protection upon
492 the injection of equal numbers of $CD4^+CD25^-$ lymphocytes into *Foxn1*^{nu} mice (**Fig. 7, D**, **E**
493 and **H**; blue bars). Conversely, a similar protection is obtained upon the immunodepletion
494 of neutrophils (**Fig. 7**, **F** and **G**) in both SCID/Beige and BALB/c mice (**Fig. 7**, **A** to **C**).

495 Taking into account the above results, we decided to investigate whether the
496 antifibrotic effects previously observed with the MMF immunosuppressant in the T cell
497 immunodeficient *Foxn1*^{nu} strain (**Fig. 3**) could also involve alterations in either the number
498 or functionality of neutrophils. We observed that the treatment with this drug does not
499 induce any significant effect in the neutrophils of *Foxn1*^{nu} mice under normal conditions.
500 However, MMF does promote a severe and systemic neutropenic effect when combined
501 with the administration of AngII (**Fig. 7I**). Taken together, these findings indicate that the
502 protective effects observed with the *Vav1* deficiency, iT_{REG} cells, and MMF against tissue
503 fibrosis can be all probably integrated in a common mechanistic framework whose final
504 end-point is the control of either tissue-resident (in the case of *Vav1*-deficient and iT_{REG}-
505 inected *WT* mice) or systemic (in the case of MMF treatments) neutrophil numbers.
506 Furthermore, they indicate that this T_{REG}/neutrophil axis confers cardiorenal protection
507 using immunosuppression-independent mechanisms.
508

509 **T_{REG} cells promote direct apoptosis of neutrophils in a CD39-dependent manner**

510 Although our results with both *Foxn1*^{nu} and SCID/Beige mice excluded the participation of
511 conventional T cells in this response, they could not formally ruled out the possibility that
512 other T_{REG} cell partners such as macrophages or dendritic cells could indirectly mediate the
513 negative effects of T_{REG} cells on neutrophil numbers. Such an idea is, in fact, consistent
514 with previous findings indicating that T_{REG} cells can mediate both acute lung injury-induced
515 fibrosis and some pathogen-triggered inflammatory responses by influencing the activity of
516 non T cell hematopoietic lineages (40, 41). To tackle this issue, we decided to investigate
517 the effect of T_{REG} cells, AngII and MMF on both neutrophil viability and function using cell
518 culture experiments. To this end, we first analyzed the effect of coculturing primary bone
519 marrow neutrophils with splenic $CD4^+CD25^+$ T cells that were directly obtained from mice
520 using flow cytometry purification procedures. These latter cells will be referred to hereafter
521 as "natural" T_{REG} (nT_{REG}) cells in order to distinguish them from the in vitro-differentiated
522 iT_{REG} cells used in previous experiments. An example of the purification of these cells can
523 be found in **Figure 8A**. These experiments revealed that neutrophils exhibit higher
524 apoptotic rates when cultured in the presence of nT_{REG} cells (**Fig. 8B**), an effect that was
525 independent on the presence of AngII in the culture media (SF, data not shown). Probably
526 as a result of this apoptotic effect, we also found that the presence of nT_{REG} cells leads to
527 the elimination of the production of reactive oxygen species (ROS) that is stimulated by
528 AngII in neutrophils (**Fig. 8C**). ROS production is mediated by the AngII AT_1 receptor in
529 neutrophils, because this response can be blocked by AT_1 (losartan), but not AT_2
530 (PD123319), receptor antagonists (**Fig. 8C**). Additional experiments indicated that nT_{REG}

cells are not exclusively involved in the negative regulation of neutrophils. For example, we observed that the supernatants from nT_{REG} cultures can promote the chemotaxis of primary neutrophils (**Fig. 8D**). All these actions seem to be nT_{REG}-specific, because no significant effects were observed when using T_H ($CD4^+$) and cytotoxic ($CD8^+$) T lymphocytes (**Fig. 8**, **B** to **D**) in these experiments. Thus, similarly to the observations made in vivo, the present results indicate that T_{REG} cells control in an AngII-independent manner the viability of primary neutrophils.

T_{REG} cells can inhibit other cell types using a number of signaling mechanisms, including CTLA4-mediated immunosuppression, granzyme and perforin-dependent cytotoxicity, cytokine-based paracrine signaling, and the degradation of extracellular ATP using the ecto-adenosine triphosphate diphosphohydrolase activity of plasma membrane-localized CD39 molecules (1, 2). We ruled out the three former mechanisms, because our results indicated that the T_{REG}/neutrophil interconnection was probably associated with an immunosuppression-independent proapoptotic mechanism (see above, **Fig. 7** and **Fig. 8B**). We also excluded a paracrine-dependent proapoptotic effect, given our observations indicating that the supernatants obtained from nT_{REG} cell cultures promote the chemotaxis rather than the apoptosis of neutrophils (**Fig. 8D**). The foregoing observations led us to consider the possible implication of CD39, a surface molecule expressed by 50 ± 7% and 58 ± 6 % of the iT_{REG} and splenic nT_{REG} cells used in this work, respectively (n = 4 independent experiments). This percentage is further expanded up to 71.7 ± 4.1% of all the iT_{REG} population when AngII is added to the in vitro T_{REG} differentiation cocktail (n = 4 independent experiments, $P \leq 0.05$). To test this idea, we purified and separated away

splenic $CD39^+$ and $CD39^-$ nT_{REG} cells by flow cytometry (**Fig. 8E**) and, subsequently, cultured them with primary bone marrow neutrophils. Using this approach, we observed that the $CD39^+$ nT_{REG} cell population, but not the $CD39^-$ one, prompts the apoptosis of neutrophils (**Fig. 8F**). This proapoptotic effect is eliminated when the ATPase activity of this ectoenzyme is blocked in those cultures with either a CD39 drug inhibitor (ARL67156; **Fig. 8F**) or excess of its normal catalytic substrate (ATP; **Fig. 8G)**. As control, no rescue is observed when the T_{REG}/neutrophil cultures are supplemented with a nonhydrolyzable form of ATP (adenosine 5'-[γ-thio]triphosphate, **Fig. 8G**). Consistent with these results, we found that ARL67156 eliminates the negative effect of nT_{REG} cells on ROS production by AngII-stimulated neutrophils (**Fig. 8C**). By contrast, ARL67156 does not block other T_{REG} cell activities, such as neutrophil chemotaxis (**Fig. 8D**). ARL57156 (**Fig. 8F**) and ATP (**Fig. 8G**) cannot prevent either the basal apoptotic rates typically exhibited by neutrophils in cell culture, further confirming that their effects are CD39-dependent.

We next investigated whether the neutropenic effect found in MMF-treated mice could be the result in some direct action of the drug on primary neutrophils. As shown in **Fig. 8H**, MMF has no effect on the viability of these cells under normal culture conditions. However, it promotes enhanced apoptotic rates when when used in AngII-stimulated neutrophil cultures (**Fig. 8H**). This goes in parallel with the elimination of ROS production by the stimulated neutrophils (**Fig. 8I**). In agreement with the stimulation-dependent effect of this drug, its proapoptotic effect is lost when the stimulated neutrophils are pretreated with losartan but not PD123319 (**Fig. 8H**). Taken together, these results indicate that the neutropenia observed in *TKO*, *Vav1*$^{-/-}$, and AngII plus MMF-treated nude mice is probably

575 due to a direct proapoptotic cell autonomous effect of both CD39$^+$ T_{REG} cells and MMF on
576 neutrophils.
577
578 **CD39$^+$ T_{REG} cells protect against AngII-driven hypertension and its comorbidities**
579 To corroborate the physiological relevance of the in vitro culture experiments described in
580 the previous section, we investigated the actual contribution of CD39$^+$ T_{REG} cells to the
581 cardiovascular and renal parameters under study in this work. To this end, we first decided
582 to analyze the effect of injecting flow cytometry-purified CD39$^+$ and CD39$^-$ iT_{REG} cells
583 (**Fig. 9A**) in the AngII-mediated fibrosis of *WT* mice. We observed that the CD39$^+$ iT_{REG}
584 subset does promote kidney neutropenia (**Fig. 9B**), protection against cardiorenal fibrosis
585 (**Fig. 9**, **C** and **D**), and the expected buffering effect on arterial blood pressure elevation
586 (**Fig. 9E**) in the recipient mice. However, such an activity was not observed when using
587 CD39$^-$ iT_{REG} cell-injected *WT* mice (**Fig. 9**, **B** to **E**). Further underscoring the role of the
588 CD39 ectoenzyme in this process, we found that the effect induced by the injected CD39$^+$
589 iT_{REG} cells is abolished when the recipient mice are treated with ARL57156 (**Fig. 9**, **B** to
590 **E**). Confirming the implication of these cells in the phenotype shown by knockout mice, we
591 found that the administration of this CD39 inhibitor to AngII-treated *Vav1*$^{-/-}$ mice
592 mimicked the effects of the T_{REG} immunodepletion previously seen in those mice, including
593 the restoration of increased numbers of kidney-resident neutrophils (**Fig. 9F**), development
594 of fibrosis in both the heart (**Fig. 9G**) and kidneys (**Fig. 9H**), elevated amounts of *Lcn2*
595 mRNA expression in kidneys (**Fig. 9I**), reductions in creatinine clearance by kidneys (**Fig.**
596 **9J**), and the restoration of a full hypertensive response (**Fig. 9K**). Collectively, these results

indicate that T_{REG} cells are involved in the protection against hypertension-driven cardiorenal fibrosis using a nonconventional, CD39- and neutrophil-dependent mechanism (**Fig. 9L**).

DISCUSSION

Our results have unveiled a hitherto unknown $CD39^+$ T_{REG} cell/neutrophil-based mechanism that probably represents a first trench of protection against AngII-elicited heart remodeling and cardiorenal fibrosis (**Fig 9L**). This mechanism has been found operative under both normotensia and hypertension conditions, suggesting that it may be involved in the homeostatic control of neutrophil numbers in some specific tissues. The utilization of a $CD39^+$ T_{REG} cell/neutrophil axis seems prima facie a good functional strategy to control these pathophysiological processes, because evidence from other fibrosis-associated kidney dysfunctions indicates that neutrophils act as critical "decision-shapers" during the inflammatory-based priming phase of the fibrotic process (8). Furthermore, they are highly dependent on both extracellular ATP and ADP availability for a large variety of functions, including survival, chemotaxis, and other proinflammatory-connected functions (42). Interestingly, this antifibrotic mechanism seems to be quite specific, as it does not confer protection under L-NAME-triggered hypertension conditions. Since *Vav1*$^{-/-}$ mice show increased T_{REG}/T_H cell ratios and neutropenia prior to the hypertension step, it is likely that this differential response could be due to the engagement of different proinflammatory or profibrotic routes upon the systemic administration of AngII and L-NAME. Likewise, we have observed that this antifibrotic mechanism does not prevent the arterial remodeling that typically develops under AngII-driven hypertension conditions. This is consistent with previous results indicating that this response may involve either macrophages or a nonconventional $CD3^+CD4^-CD8^-$ T cell subpopulation (15, 20).

622 It is worth noting that this new regulatory layer involved in fibrotic responses does
623 not exclude the participation of T_H cells and other myeloid cells further downstream in the
624 fibrotic pathophysiological cascade. On the contrary, our observations suggest that this first
625 T_{REG}-dependent barrier of defense against AngII-driven tissue fibrosis is probably
626 overcome under chronic hypertension conditions by the subsequent recruitment and/or
627 activation of either T_H cell subtypes or downstream proinflammatory responses providing
628 that normal T_{REG}/T_H ratios are preserved in mice (**Fig. 9L**). In any case, the protection
629 shown by T_{REG} cell-transplanted *WT* mice suggests that therapies based on either alterations
630 of T_{REG}/T_H cell ratios (i.e., via either allogenic T_{REG} cell transfer or in vivo expansion of
631 T_{REG} cells) or ATP/ADP depletion-dependent reduction of neutrophil numbers (i.e., using
632 recombinant CD39 delivery techniques) could be valuable, either singlehandedly or in
633 combination with AngII route inhibitors, to prevent cardiorenal fibrosis and the ensuing
634 end-organ disease in patients with AngII-dependent hypertension.

635 Our results also suggest that previous findings regarding the positive effect of MMF
636 and other immunosuppressants in hypertension-driven fibrosis (12, 13, 21) can be
637 explained by the enhancement of this T_{REG}-dependent mechanism. Consistent with this, it
638 has been shown that some of those immunosupressants promote the peripheral expansion of
639 T_{REG} cells (43, 44). The mechanism reported here could be also involved in both the fibrotic
640 and hypertensive effects induced by either the transplantation and depletion of both
641 conventional T and T_{REG} cells due to the changes in T_{REG}/T_H ratios intrinsically associated
642 with these treatments (9, 10, 15-17). Interestingly, it has been reported that the MMF
643 treatment promotes neutropenia in some tissue-transplanted patients (45-47). Based on the

644 present results, it would be interesting to verify whether this collateral effect could be
645 caused by a similar mechanism to the one described here. It would be also worth pursuing a
646 better understanding of the proapoptotic effect of MMF on neutrophils. Given that this
647 effect is only observed in an AngII- and AT_1 receptor-dependent manner, we surmise that
648 MMF must create some metabolic imbalance in stimulated neutrophils. Whether this is
649 done via in-target (inhibition of inosine monophosphate dehydrogenase) or off-target
650 effects of the drug, remains to be determined. Effects of MMF in non lymphoid cells have
651 been previously described (39).

652 Interestingly, we have observed that the lack of tissue fibrosis found in *TKO* and
653 *Vav1*$^{-/-}$ mice is always associated with the development of milder hypertensive states
654 during AngII-driven hypertension conditions (**Fig. 9L**). Our interpretation is that this latter
655 effect is a downstream consequence of the lack of fibrosis and the subsequent preservation
656 of normal renal functions in these mice. However, given the highly intertwined connections
657 between these two pathophysiological programs, it could be also argued that the mild
658 hypertensive conditions are in fact responsible for the antifibrotic protection exhibited by
659 these two mouse strains. Although it is difficult to formally exclude this possibility at the
660 experimental level, we do not believe this alternative scenario is possible because: **(i)** We
661 have observed that the arterial blood pressure of AngII-infused *WT* and *Vav1*$^{-/-}$ mice is
662 rather similar during the early phases of the AngII infusion (0 to six weeks) and only
663 become statistically different upon the long-term exposure of animals to this vasopressor
664 (10-15 weeks). Thus, from a kinetic point of view, it does not seem that the differential
665 hypertension values could be the original cause of the lack of fibrosis in Vav1-deficient

mice. **(ii)** We have found that the overall blood pressure levels shown by AngII-infused *Vav1*$^{-/-}$ and *TKO* mice are similar to those present in animals that do develop a full fibrotic response (i.e., untreated *DKO* mice). Consistent with this, we also have found that *TKO* (both untreated and AngII-treated) and *Vav1*$^{-/-}$ (AngII treated) mice do develop other hypertension-associated dysfunctions such as, for example, the thickening of the arterial media wall. **(iii)** We have seen that the time of divergence of blood pressure values between AngII-infused *WT* and *Vav1*$^{-/-}$ mice matches the time when the controls have already developed cardiorenal fibrosis (**Fig. 2H**), thus suggesting that the milder hypertension shown by untreated *TKO*, AngII-treated *TKO*, and AngII-infused *Vav1*$^{-/-}$ mice could be an effect derived from the lack of fibrosis development in these animals. This could originate from either a direct pressor effect of the lack of fibrosis or by the collateral engagement of other hypertension-linked processes that contribute to the pressure-natriuresis mechanism involved in long-term pressure control (i.e., production of aldosterone and vasopressin) (48). Regardless of the initial cause of the event, it is clear that the renal dysfunctions and the hypertensive state will eventually collaborate in a mutually reinforcing loop to ultimately determine the final arterial pressure and fibrosis state found in each of the control and test strains analyzed in the present study.

Outside the cardiovascular field, this work has also given information about the role of Vav proteins in lymphocyte subpopulations and neutrophils. Thus, we have observed that Vav proteins seem to be dispensable for both T_{REG} cell development and effector functions at least in the pathophysiological context studied in this work. This is in sharp contrast to the critical roles played by these proteins during the stepwise development,

688 selection, and final effector stages of conventional $CD4^+$ and $CD8^+$ T cells (27, 28). Given
689 that T_{REG} cells require low T cell receptor signals to undergo effective positive selection
690 (49), this result suggests that Vav proteins probably contribute to establish optimal
691 thresholds of T cell receptor signaling during the intrathymic selection process rather being
692 involved in yes/no digital decisions. The increased T_{REG}/T_H cell ratios present in these mice
693 may also explain the lack of autoimmunity present in Vav family deficient mice despite
694 their defects in negative selection (50). Such property is specific for Vav proteins, because
695 the elimination of other proximal T cell receptor signaling elements such as Zap70 and Lat
696 does block T_{REG} cell development in the thymus (51, 52). We have also seen that the lack of
697 Vav1 does not seem to significantly affect the overall functionality of neutrophils.
698 Consistent with this, we have observed that the renal neutropenia found in these mice can
699 be restored upon the immunodepletion of iT_{REG} cells. Conversely, a similar neutropenic
700 effect can be induced when *WT* mice are injected with iT_{REG} cells. Additional experiments
701 have also revealed that the AngII-stimulation of neutrophil migration and ROS production
702 is Vav1-independent (SF, unpublished data). These data are in agreement with previous
703 results from H. Welch' lab indicating no major defects in the in vivo biological properties
704 of *Vav1*$^{-/-}$ neutrophils (53, 54). It would be important, in any case, to continue the analyses
705 of *Vav1*$^{-/-}$ T_{REG} cells and neutrophils to assess whether this protein plays some catalysis-
706 dependent or independent roles in any of these cell types.

707 Taken together, these results provide a new biological perspective to understand the
708 early steps involved in the ontogeny of cardiorenal fibrosis, one of the most fatal
709 comorbidities associated with essential hypertension (5, 6). Given that other fibrotic- or

710 T_{REG} cell -dependent diseases in liver, lung, and muscle are influenced by AngII (8, 37), it
711 would be interesting to investigate whether the T_{REG} cell/neutrophil axis reported here could
712 also play protective roles against those conditions.
713

ACKNOWLEDGEMENTS

We thank A. Abad, M. Blázquez, and personnel of the CIC Microscopy, Pathology, and Cytometry units for technical assistance, Dr. M. Dosil for comments on the manuscript, and Drs. V. Tybulewicz and M. Turner for making available to us the initial stocks of *Vav1* and *Vav2* knockout mice, respectively. This work has been supported by grants from the Castilla-León Autonomous Government (CSI101U13) the Spanish Ministry of Economy and Competitiveness (SAF2012-31371, RD12/0036/0002), Worldwide Cancer Research, the Solórzano Foundation, and the Ramón Areces Foundation to XRB. PM funding is from the Spanish Ministry of Economy and Competitiveness (SAF2011-27330). SF, MM-M, JR-V, and AM-M were supported by the Spanish Ministry of Economy and Competitiveness through BES-2010-031386, CSIC JAE-Doc, Juan de la Cierva, and BES-2009-016103 contracts, respectively. Spanish government-sponsored funding to XRB is partially supported by the European Regional Development Fund.

COMPETING INTERESTS

None.

AUTHOR CONTRIBUTIONS

SF participated in all the experimental work, analyzed data, and contributed to artwork design and manuscript writing. MM-M performed animal-based work, designed experiments, and analyzed data. JR-V analyzed flow cytometry data and carried out histochemical analyses. MP and JML-N performed experiments related to in vivo renal functions. MAS and MJA collaborated in blood pressure determination experiments. AM-

737 M and PM carried out work related to the characterization of kidney-resident hematopoietic
738 cells. CG-M performed and analyzed immunohistochemical analyses in tissue sections. BA
739 helped in cell transplantation experiments with Ly5 mice. XRB designed the work,
740 analyzed data, wrote the manuscript, and carried out the final editing of figures.
741

REFERENCES

1. **Josefowicz SZ, Lu LF, Rudensky AY.** 2012. Regulatory T cells: mechanisms of differentiation and function. Annu Rev Immunol **30:**531-564.
2. **Shevach EM.** 2009. Mechanisms of foxp3+ T regulatory cell-mediated suppression. Immunity **30:**636-645.
3. **Burzyn D, Benoist C, Mathis D.** 2013. Regulatory T cells in nonlymphoid tissues. Nat Immunol **14:**1007-1013.
4. **Burzyn D, Kuswanto W, Kolodin D, Shadrach JL, Cerletti M, Jang Y, Sefik E, Tan TG, Wagers AJ, Benoist C, Mathis D.** 2013. A special population of regulatory T cells potentiates muscle repair. Cell **155:**1282-1295.
5. **Kearney PM, Whelton M, Reynolds K, Muntner P, Whelton PK, He J.** 2005. Global burden of hypertension: analysis of worldwide data. Lancet **365:**217-223.
6. **Lopez AD, Mathers CD, Ezzati M, Jamison DT, Murray CJ.** 2006. Global and regional burden of disease and risk factors, 2001: systematic analysis of population health data. Lancet **367:**1747-1757.
7. **Liu Y.** 2011. Cellular and molecular mechanisms of renal fibrosis. Nat Rev Nephrol **7:**684-696.
8. **Wynn TA, Ramalingam TR.** 2012. Mechanisms of fibrosis: therapeutic translation for fibrotic disease. Nat Med **18:**1028-1040.
9. **Kvakan H, Kleinewietfeld M, Qadri F, Park JK, Fischer R, Schwarz I, Rahn HP, Plehm R, Wellner M, Elitok S, Gratze P, Dechend R, Luft FC, Muller DN.** 2009.

763 Regulatory T cells ameliorate angiotensin II-induced cardiac damage. Circulation
764 **119:**2904-2912.
765 10. **Barhoumi T, Kasal DA, Li MW, Shbat L, Laurant P, Neves MF, Paradis P,**
766 **Schiffrin EL.** 2011. T regulatory lymphocytes prevent angiotensin II-induced
767 hypertension and vascular injury. Hypertension **57:**469-476.
768 11. **Kasal DA, Barhoumi T, Li MW, Yamamoto N, Zdanovich E, Rehman A, Neves**
769 **MF, Laurant P, Paradis P, Schiffrin EL.** 2011. T regulatory lymphocytes prevent
770 aldosterone-induced vascular injury. Hypertension **59:**324-330.
771 12. **Muller DN, Shagdarsuren E, Park JK, Dechend R, Mervaala E, Hampich F,**
772 **Fiebeler A, Ju X, Finckenberg P, Theuer J, Viedt C, Kreuzer J, Heidecke H,**
773 **Haller H, Zenke M, Luft FC.** 2002. Immunosuppressive treatment protects against
774 angiotensin II-induced renal damage. Am J Pathol **161:**1679-1693.
775 13. **Crowley SD, Frey CW, Gould SK, Griffiths R, Ruiz P, Burchette JL, Howell DN,**
776 **Makhanova N, Yan M, Kim HS, Tharaux PL, Coffman TM.** 2008. Stimulation of
777 lymphocyte responses by angiotensin II promotes kidney injury in hypertension. Am J
778 Physiol Renal Physiol **295:**F515-524.
779 14. **Mervaala E, Muller DN, Park JK, Dechend R, Schmidt F, Fiebeler A, Bieringer**
780 **M, Breu V, Ganten D, Haller H, Luft FC.** 2000. Cyclosporin A protects against
781 angiotensin II-induced end-organ damage in double transgenic rats harboring human
782 renin and angiotensinogen genes. Hypertension **35:**360-366.

15. **Guzik TJ, Hoch NE, Brown KA, McCann LA, Rahman A, Dikalov S, Goronzy J, Weyand C, Harrison DG.** 2007. Role of the T cell in the genesis of angiotensin II induced hypertension and vascular dysfunction. J Exp Med **204:**2449-2460.

16. **Madhur MS, Lob HE, McCann LA, Iwakura Y, Blinder Y, Guzik TJ, Harrison DG.** 2010. Interleukin 17 promotes angiotensin II-induced hypertension and vascular dysfunction. Hypertension **55:**500-507.

17. **Shao J, Nangaku M, Miyata T, Inagi R, Yamada K, Kurokawa K, Fujita T.** 2003. Imbalance of T-cell subsets in angiotensin II-infused hypertensive rats with kidney injury. Hypertension **42:**31-38.

18. **Crowley SD, Song YS, Lin EE, Griffiths R, Kim HS, Ruiz P.** 2010. Lymphocyte responses exacerbate angiotensin II-dependent hypertension. Am J Physiol Regul Integr Comp Physiol **298:**R1089-1097.

19. **Harrison DG, Guzik TJ, Lob HE, Madhur MS, Marvar PJ, Thabet SR, Vinh A, Weyand CM.** 2011. Inflammation, immunity, and hypertension. Hypertension **57:**132-140.

20. **Rodriguez-Iturbe B, Pons H, Herrera-Acosta J, Johnson RJ.** 2001. Role of immunocompetent cells in nonimmune renal diseases. Kidney Int **59:**1626-1640.

21. **Rodriguez-Iturbe B, Pons H, Quiroz Y, Gordon K, Rincon J, Chavez M, Parra G, Herrera-Acosta J, Gomez-Garre D, Largo R, Egido J, Johnson RJ.** 2001. Mycophenolate mofetil prevents salt-sensitive hypertension resulting from angiotensin II exposure. Kidney Int **59:**2222-2232.

22. **McMaster WG, Kirabo A, Madhur MS, Harrison DG.** 2015. Inflammation, immunity, and hypertensive end-organ damage. Circ Res **116:**1022-1033.

23. **Bustelo XR.** 2000. Regulatory and signaling properties of the Vav family. Mol Cell Biol **20:**1461-1477.

24. **Bustelo XR.** 2014. Vav family exchange factors: an integrated regulatory and functional view. Small GTPases **5:**1-12.

25. **Turner M, Billadeau DD.** 2002. VAV proteins as signal integrators for multi-subunit immune-recognition receptors. Nat Rev Immunol **2:**476-486.

26. **Tarakhovsky A, Turner M, Schaal S, Mee PJ, Duddy LP, Rajewsky K, Tybulewicz VL.** 1995. Defective antigen receptor-mediated proliferation of B and T cells in the absence of Vav. Nature **374:**467-470.

27. **Turner M, Mee PJ, Walters AE, Quinn ME, Mellor AL, Zamoyska R, Tybulewicz VL.** 1997. A requirement for the Rho-family GTP exchange factor Vav in positive and negative selection of thymocytes. Immunity **7:**451-460.

28. **Fujikawa K, Miletic AV, Alt FW, Faccio R, Brown T, Hoog J, Fredericks J, Nishi S, Mildiner S, Moores SL, Brugge J, Rosen FS, Swat W.** 2003. Vav1/2/3-null mice define an essential role for Vav family proteins in lymphocyte development and activation but a differential requirement in MAPK signaling in T and B cells. J Exp Med **198:**1595-1608.

29. **Sauzeau V, Sevilla MA, Rivas-Elena JV, de Alava E, Montero MJ, Lopez-Novoa JM, Bustelo XR.** 2006. Vav3 proto-oncogene deficiency leads to sympathetic hyperactivity and cardiovascular dysfunction. Nat Med **12:**841-845.

30. **Sauzeau V, Jerkic M, Lopez-Novoa JM, Bustelo XR.** 2007. Loss of Vav2 proto-oncogene causes tachycardia and cardiovascular disease in mice. Mol Biol Cell **18:**943-952.

31. **Sauzeau V, Horta-Junior JAC, Riolobos AS, Fernandez G, Sevilla MA, Lopez DE, Montero MJ, Rico B, Bustelo XR.** 2010. Vav3 is involved in GABAergic axon guidance events important for the proper function of brainstem neurons controlling cardiovascular, respiratory, and renal parameters. Mol Biol Cell **21:**4251-4263.

32. **Sauzeau V, Sevilla MA, Montero MJ, Bustelo XR.** 2010. The Rho/Rac exchange factor Vav2 controls nitric oxide-dependent responses in mouse vascular smooth muscle cells. J Clin Invest **120:**315-330.

33. **Jonsson CA, Svensson L, Carlsten H.** 1999. Beneficial effect of the inosine monophosphate dehydrogenase inhibitor mycophenolate mofetil on survival and severity of glomerulonephritis in systemic lupus erythematosus (SLE)-prone MRLlpr/lpr mice. Clin Exp Immunol **116:**534-541.

34. **Kassan M, Montero MJ, Sevilla MA.** 2010. In vitro antioxidant activity of pravastatin provides vascular protection. Eur J Pharmacol **630:**107-111.

35. **Menacho-Marquez M, Garcia-Escudero R, Ojeda V, Abad A, Delgado P, Costa C, Ruiz S, Alarcon B, Paramio JM, Bustelo XR.** 2013. The Rho exchange factors Vav2 and Vav3 favor skin tumor initiation and promotion by engaging extracellular signaling loops. PLoS Biol **11:**e1001615.

36. **Paragas N, Qiu A, Hollmen M, Nickolas TL, Devarajan P, Barasch J.** 2012. NGAL-Siderocalin in kidney disease. Biochim Biophys Acta **1823:**1451-1458.

37. **Benigni A, Cassis P, Remuzzi G.** 2010. Angiotensin II revisited: new roles in inflammation, immunology and aging. EMBO Mol Med **2:**247-257.

38. **Rees DD, Palmer RM, Hodson HF, Moncada S.** 1989. A specific inhibitor of nitric oxide formation from L-arginine attenuates endothelium-dependent relaxation. Br J Pharmacol **96:**418-424.

39. **Sintchak MD, Nimmesgern E.** 2000. The structure of inosine 5'-monophosphate dehydrogenase and the design of novel inhibitors. Immunopharmacology **47:**163-184.

40. **D'Alessio FR, Tsushima K, Aggarwal NR, West EE, Willett MH, Britos MF, Pipeling MR, Brower RG, Tuder RM, McDyer JF, King LS.** 2009. CD4+CD25+Foxp3+ Tregs resolve experimental lung injury in mice and are present in humans with acute lung injury. J Clin Invest **119:**2898-2913.

41. **Lewkowicz P, Lewkowicz N, Sasiak A, Tchorzewski H.** 2006. Lipopolysaccharide-activated CD4+CD25+ T regulatory cells inhibit neutrophil function and promote their apoptosis and death. J Immunol **177:**7155-7163.

42. **Junger WG.** 2011. Immune cell regulation by autocrine purinergic signalling. Nat Rev Immunol **11:**201-212.

43. **Noris M, Casiraghi F, Todeschini M, Cravedi P, Cugini D, Monteferrante G, Aiello S, Cassis L, Gotti E, Gaspari F, Cattaneo D, Perico N, Remuzzi G.** 2007. Regulatory T cells and T cell depletion: role of immunosuppressive drugs. J Am Soc Nephrol **18:**1007-1018.

44. **Barrat FJ, Cua DJ, Boonstra A, Richards DF, Crain C, Savelkoul HF, de Waal-Malefyt R, Coffman RL, Hawrylowicz CM, O'Garra A.** 2002. In vitro generation of

870 interleukin 10-producing regulatory CD4(+) T cells is induced by immunosuppressive
871 drugs and inhibited by T helper type 1 (Th1)- and Th2-inducing cytokines. J Exp Med
872 **195:**603-616.
873 45. **Hafiz MM, Faradji RN, Froud T, Pileggi A, Baidal DA, Cure P, Ponte G, Poggioli**
874 **R, Cornejo A, Messinger S, Ricordi C, Alejandro R.** 2005. Immunosuppression and
875 procedure-related complications in 26 patients with type 1 diabetes mellitus receiving
876 allogeneic islet cell transplantation. Transplantation **80:**1718-1728.
877 46. **Banerjee R, Halil O, Bain BJ, Cummins D, Banner NR.** 2000. Neutrophil dysplasia
878 caused by mycophenolate mofetil. Transplantation **70:**1608-1610.
879 47. **Nogueras F, Espinosa MD, Mansilla A, Torres JT, Cabrera MA, Martin-Vivaldi**
880 **R.** 2005. Mycophenolate mofetil-induced neutropenia in liver transplantation.
881 Transplant Proc **37:**1509-1511.
882 48. **Cowley AW, Jr.** 1992. Long-term control of arterial blood pressure. Physiol Rev
883 **72:**231-300.
884 49. **Hwang S, Song KD, Lesourne R, Lee J, Pinkhasov J, Li L, El-Khoury D, Love PE.**
885 2012. Reduced TCR signaling potential impairs negative selection but does not result in
886 autoimmune disease. J Exp Med **209:**1781-1795.
887 50. **Ruiz S, Santos E, Bustelo XR.** 2009. The use of knockout mice reveals a synergistic
888 role of the Vav1 and Rasgrf2 gene deficiencies in lymphomagenesis and metastasis.
889 PLoS One **4:**e8229.
890 51. **Sommers CL, Lee J, Steiner KL, Gurson JM, Depersis CL, El-Khoury D, Fuller**
891 **CL, Shores EW, Love PE, Samelson LE.** 2005. Mutation of the phospholipase C-

gamma1-binding site of LAT affects both positive and negative thymocyte selection. J Exp Med **201:**1125-1134.

52. **Sakaguchi N, Takahashi T, Hata H, Nomura T, Tagami T, Yamazaki S, Sakihama T, Matsutani T, Negishi I, Nakatsuru S, Sakaguchi S.** 2003. Altered thymic T-cell selection due to a mutation of the ZAP-70 gene causes autoimmune arthritis in mice. Nature **426:**454-460.

53. **Pan D, Amison RT, Riffo-Vasquez Y, Spina D, Cleary SJ, Wakelam MJ, Page CP, Pitchford SC, Welch HC.** 2015. P-Rex and Vav Rac-GEFs in platelets control leukocyte recruitment to sites of inflammation. Blood **125:**1146-1158.

54. **Lawson CD, Donald S, Anderson KE, Patton DT, Welch HC.** 2011. P-Rex1 and Vav1 cooperate in the regulation of formyl-methionyl-leucyl-phenylalanine-dependent neutrophil responses. J Immunol **186:**1467-1476.

905 **TABLE 1.** Percentage of hematopoietic subpopulations in mice of indicated genotypes.
906

Tissue	Cell type	Mouse genotype			
		WT	***DKO***	***TKO***	***Vav1*$^{-/-}$**
Kidney	$CD11b^+Gr1^+$ neutrophils	0.37±0.07	**0.91±0.17***	**0.1±0.03***,†	**0.15±0.01***,†
	$CD4^+$ T cells	0.14±0.02[a]	0.13±0.01	**0.02±0.005***,†	**0.02±0.000***,†
	$CD4^+Foxp3^+$ T_{REG} cells	0.06±0.03	0.07±0.02	0.02±0.003	0.01±0.002
	$CD11b^+F4/80^+$ macrophages	0.69±0.16	0.73±0.11	0.45±0.07	ND
	$CD11c^+$ dendritic cells	0.26±0.04	0.26±0.04	0.3±0.03	ND
	$CD11c^-$ dendritic cells	0.16±0.04	0.17±0.05	0.14±0.03	ND
	$CD8^+$ T cells	0.60±0.06	0.68±0.047	0.643±0.031	ND
	$B220^+$ B cells	18.80±1.09	18.98±1.75	18.467±2.17	ND
Blood	$CD11b^+Gr1^+$ neutrophils	18.30±2.6	**48.20±2.60***	**46.3±7***,†	12.1±1.3
	$CD4^+$ T cells	22.08±2.11	29.24±3.10	**7.43±0.14***,†	**5.73±0.21***,†
	$CD4^+Foxp3^+$ T_{REG} cells	1.22±0.21	2.46±0.36	1.63	1.35±0.04
	$CD8^+$ T cells	16.07±0.91	7.67±1.94	**4.03±1.35***,†	**6.09±0.72***,†
	$B220^+$ B cells	29.25±9.33	**12.24±3.65***	**7.92±2.01***	**7.34±2.96***
Spleen	$CD4^+$ T cells	10.07±0.48	12.17±1.67	**3.77±0.44***,†	**4.35±0.32***,†
	$CD4^+Foxp3^+$ T_{REG} cells	1.04±0.065	0.95±0.02	0.91±0.02	1.11±0.079
	$CD8^+$ T cells	10.60±0.69	8.52±0.37	**3.43±0.49***,†	**3.41±0.17***,†
	$B220^+$ B cells	70.25±1.19	71.4±1.9	**33.7±2.84***,†	**26.2±3.08***,†
Thymus	$CD4^+CD8^-$ T cells	9.71±0.53	9.34±0.64	**2.77±0.25***,†	**5.21±1.07***,†
	$CD4^+Foxp3^+$ T_{REG} cells	0.49±0.04	0.39±0.06	0.29±0.06	0.6±0.18
	$CD4^-CD8^+$ T cells	6.57±2.03	2.93±0.32	**1.8±0.19***,†	**3.39±0.68***,†
	$CD4^+CD8^+$ thymocytes	75.3±1.96	80.5±1	**40.23±1.52***,†	**59.3±5.57***,†
	$CD4^-CD8^-$ thymocytes	8.24±0.86	7.24±0.3	**55.17±1.52***,†	**31.6±5.16***,†

907 [a] Percentage (in %) of indicated cells in the total population analyzed were measured by
908 flow cytometry as indicated in Experimental Procedures. Statistically significant
909 variations are shown using red bold type. * and †, $P \leq 0.05$ relative to *WT* and *DKO* mice,
910 respectively ($n = 6$ mice/genotype). ND, not determined.
911

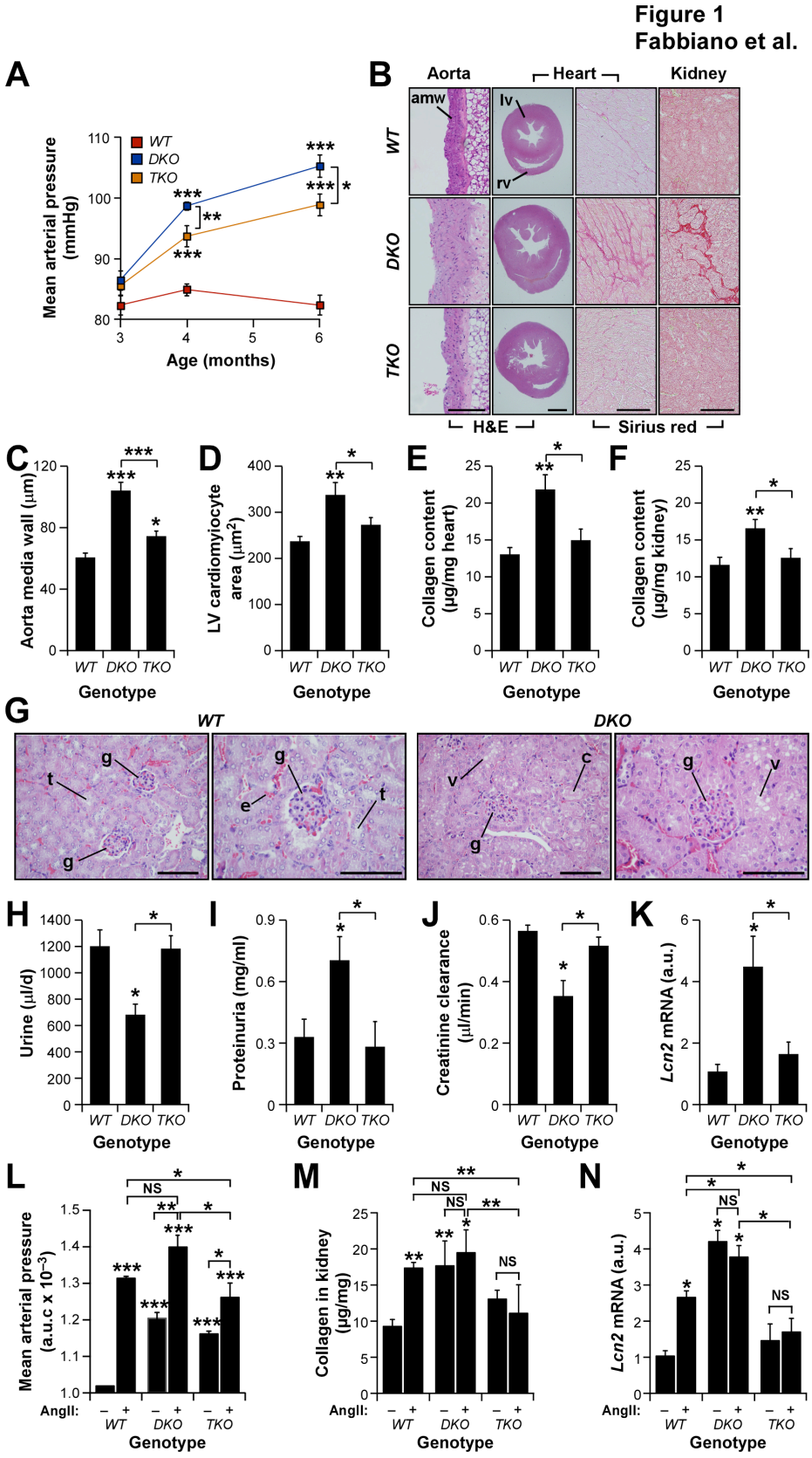
Figure 1
Fabbiano et al.
A
Mean arterial pressure (mmHg)
Age (months)
WT
DKO
TKO
B
Aorta
Heart
Kidney
amw
lv
rv
H&E
Sirius red
C
Aorta media wall (μm)
D
LV cardiomyiocyte area (μm²)
E
Collagen content (μg/mg heart)
F
Collagen content (μg/mg kidney)
Genotype
G
WT
DKO
H
Urine (μl/d)
I
Proteinuria (mg/ml)
J
Creatinine clearance (μl/min)
K
Lcn2 mRNA (a.u.)
L
Mean arterial pressure (a.u.c x 10⁻³)
AngII:
M
Collagen in kidney (μg/mg)
N
Lcn2 mRNA (a.u.)
NS

913 **FIGURE 1.** Vav family *TKO* mice show protection against heart hypertrophy and
914 cardiorenal fibrosis. **(A)** Mean arterial pressure evolution in indicated mice. *, $P \leq 0.05$;
915 ***, $P \leq 0.001$ ($n = 8$). **(B)** Examples of aorta (left panels), heart ventricles (second panels
916 from left), left ventricle (third panels from left) and kidney (right panels) sections obtained
917 from four-month-old mice of indicated genotypes (left). Sections were stained as indicated
918 (bottom). Sirius-red-stained fibrotic deposits in interstitial areas are seen as dark pink areas
919 (fourth panel from left). amw, aorta media wall; lv, left ventricle; rv, right ventricle. Scale
920 bars, 100 μm. Similar results were obtained using serial sections and independent mice ($n =$
921 4). **(C** to **F)** Status of cardiovascular (C and D) and cardiorenal (E and F) parameters in
922 mice of indicated genotypes. LV, left ventricle. *, $P \leq 0.05$; **, $P \leq 0.01$; ***, $P \leq 0.001$
923 relative to either control or indicated experimental pair (in brackets) ($n = 4$). **(G)** Example
924 of kidney sections from mice of indicated genotypes (top). *WT* mice exhibit normal
925 glomeruli (g) and tubules (t) whereas DKO animals display typical signs of glomerular
926 sclerosis, cytoplasmic vacuolar accumulation (v) in necrotic tubules, and protein casts (c).
927 Erithrocytes (e) are seen as red spots in all sections. Scale bars, 50 μm. **(H** to **J)** Daily urine
928 production (H, $n = 6$), urine protein content (I, $n = 6$), and creatinine clearance rates (J, $n =$
929 4) in mice of indicated genotypes. *, $P \leq 0.05$ relative to either control or indicated
930 experimental pair (in brackets). **(K)** Levels of *Lcn2* transcript in kidneys of indicated
931 animals. *, $P \leq 0.05$ relative to either control or indicated experimental pair (in brackets) (n
932 = 4). **(L** to **N)** Area under the curve (a.u.c.) values (L) and renal parameters (M and N) in
933 mice of indicated genotypes after being infused with (+) or without (–) AngII. *, $P \leq 0.05$;
934 **, $P \leq 0.01$; ***, $P \leq 0.001$ relative to either control or indicated experimental pairs (in

935 brackets) (n = 4). NS, not statistically significant. Error bars in panels of this figure and
936 subsequent ones represent the S.E.M.
937

938

Figure 2
Fabbiano et al.

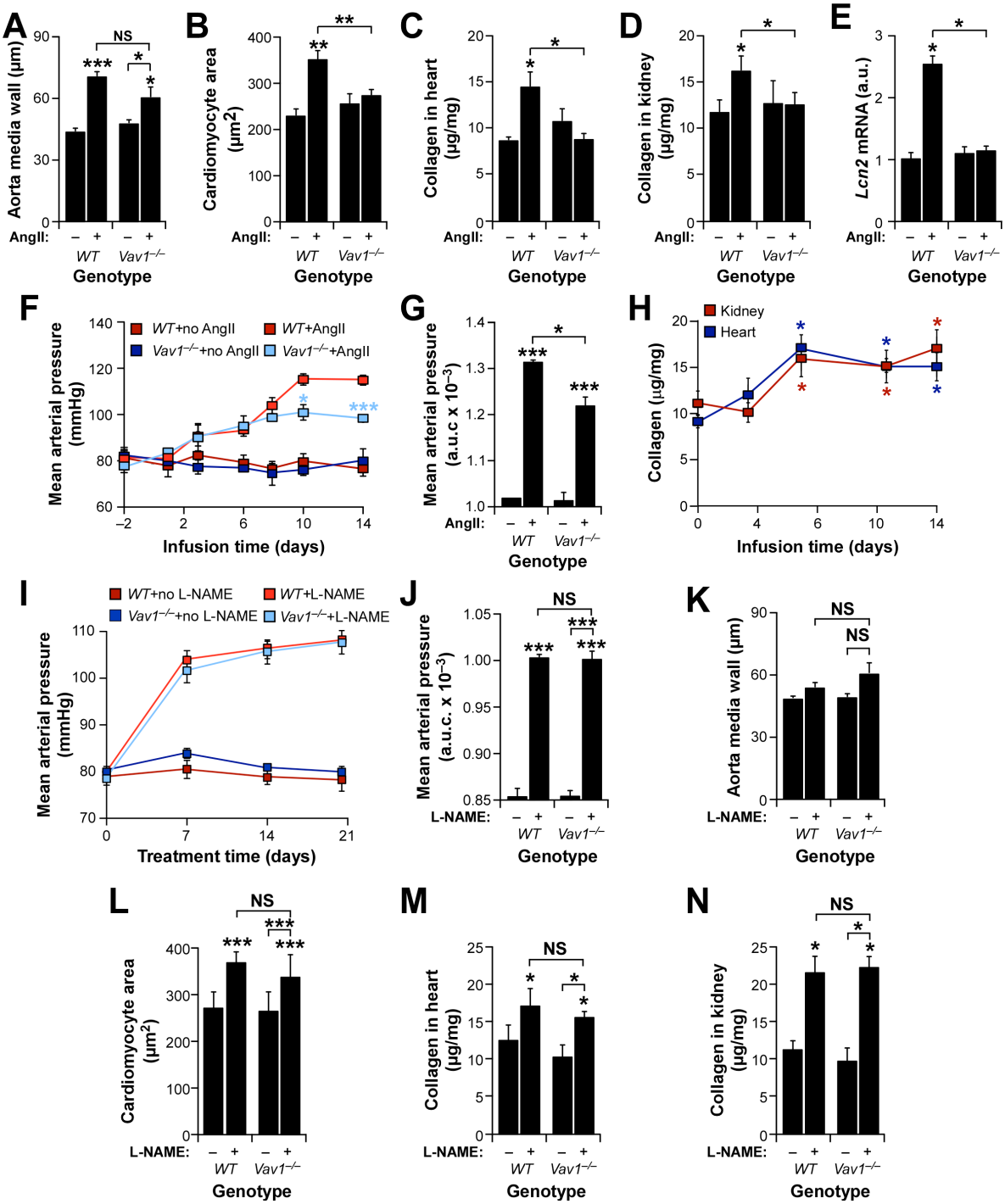

939

940

941 **FIGURE 2.** The *Vav1* gene deficiency protects against AngII-triggered cardiorenal
942 dysfunctions. **(A** to **E)** Status of indicated cardiovascular (A to C) and renal (D and E)
943 parameters in mice of indicated genotypes after being infused with (+) or without (–)
944 AngII. *, $P \leq 0.05$; **, $P \leq 0.01$; ***, $P \leq 0.001$ ($n = 10$). **(F** and **G)** Mean arterial pressure
945 evolution (F) and a.u.c. values (G) in indicated mouse strains and treatments. *, $P \leq 0.05$;
946 ***, $P \leq 0.001$ ($n = 6$). **(H)** Kinetics of cardiorenal fibrosis development in AngII-treated
947 *WT* mice. *, $P \leq 0.05$ ($n = 4$). **(I** and **J)** Evolution (I) and a.u.c. (J) of mean arterial pressure
948 in mice of indicated genotypes in the presence or absence of L-NAME. ***, $P \leq 0.001$ ($n =$
949 4). **(K** to **N)** Status of indicated vascular (K), heart (L,M) and renal (N) parameters in *WT*
950 and *Vav1*$^{-/-}$ mice at the end of L-NAME treatments. Please note that, unlike the case of
951 AngII infusion, the oral administration of L-NAME does not induce aorta remodeling even
952 in *WT* mice (K). *, $P \leq 0.05$; ***, $P \leq 0.001$ ($n = 4$). Statistical values are given relative to
953 either untreated *WT* controls or indicated experimental pairs (in brackets).
954

955

956

957

958

959

Figure 3
Fabbiano et al.

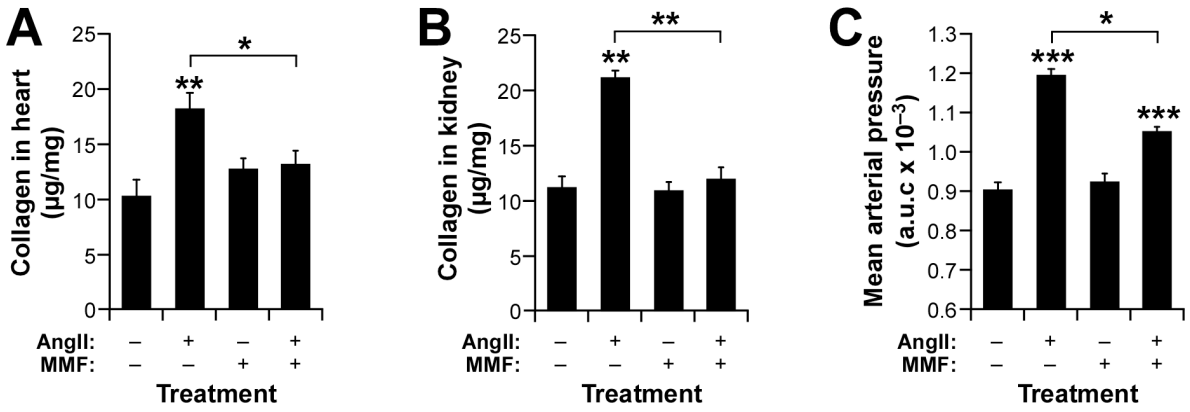

960

961

962 **FIGURE 3.** MMF protects immunodeficient mice against cardiorenal fibrosis. **(A** to **B)**
963 Cardiorenal fibrosis (A and B) and a.u.c. blood pressure levels (C) developed by *Foxn1*^{nu}
964 mice after a 14-day-long treatment with indicated agents (bottom) *, $P \leq 0.05$; **, $P \leq 0.01$;
965 ***, $P \leq 0.001$ relative to either control or indicated experimental pairs (in brackets) (n =
966 6).

967

Figure 4
Fabbiano et al.

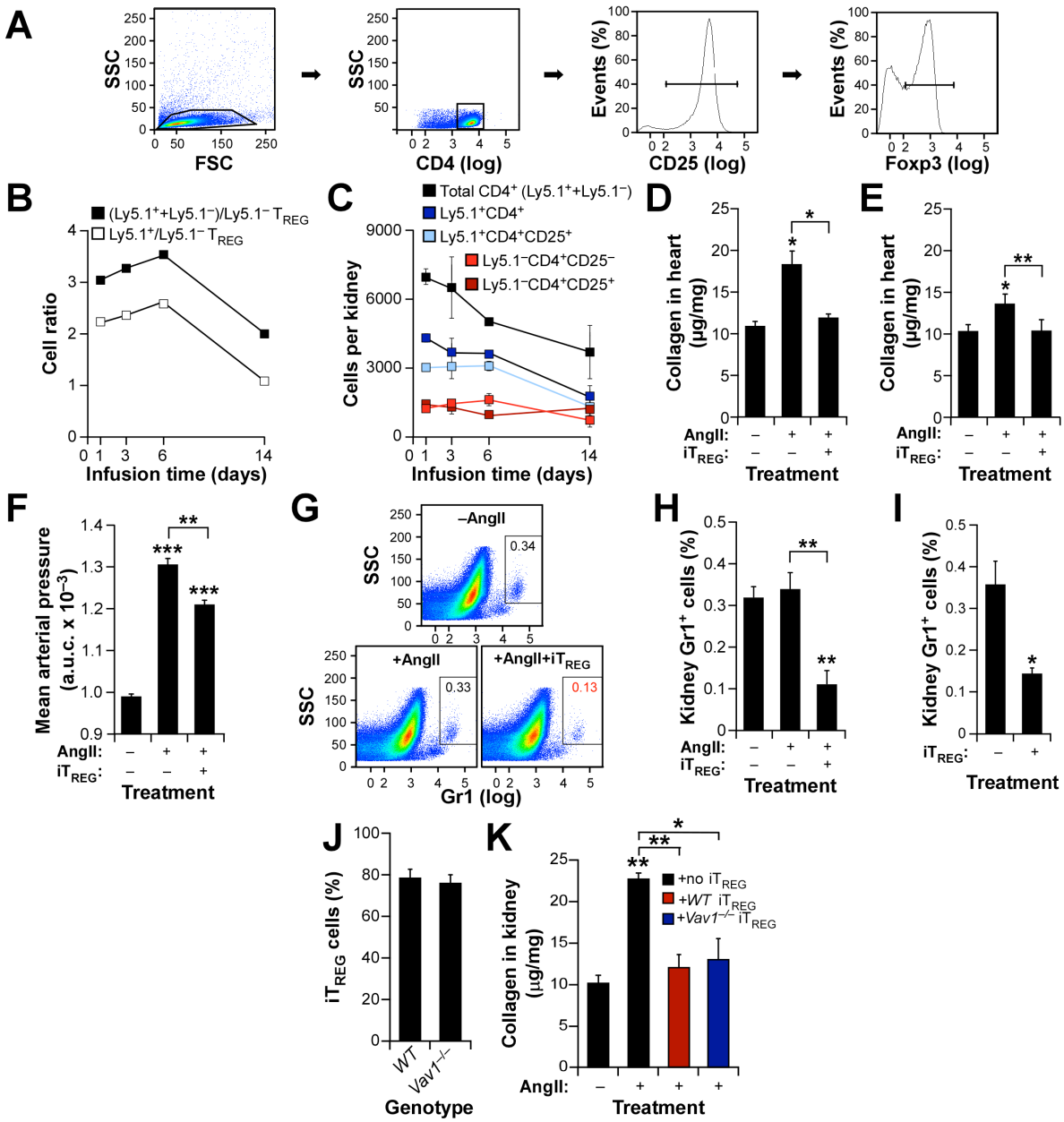

FIGURE 4. Increased T_{REG}/T_H cell percentages protect against AngII-triggered cardiorenal fibrosis. **(A)** Example of purified iT_{REG} cells used in these experiments. $CD4^+$ cells obtained from homogenized spleens and separated by flow cytometry (two left panels) were cultured with antibodies to CD3 and CD28, interleukin 2 and transforming growth factor β_1. After

four days, CD25 expression was checked by flow cytometry (third panel from left) and injected into mice. Aliquots of cells were in some cases checked for Foxp3 expression (right). **(B)** Ratio of indicated cell populations in kidneys from animals that, upon injection of 2 x 10^5 Lyt.1$^+$ T_{REG} cells, were infused 24 hours later with AngII for the indicated periods of time. **(C)** Mean number of indicated cell populations found in kidneys from mice used in panel B (n = 4). **(D** to **F)** Cardiorenal fibrosis (D and E) and a.u.c. mean arterial pressure levels (F) present in *WT* mice that had been maintained under the indicated conditions for 14 days, *, $P \leq 0.05$; **, $P \leq 0.01$; ***, $P \leq 0.001$ relative to either control or indicated experimental pairs (in brackets) (n = 4). **(G** and **H)** Representative example (G) and quantification (H) of kidney-resident neutrophils in kidneys from *WT* mice at the end of the above experiments. **, $P \leq 0.01$ relative to either control or indicated experimental pairs (in brackets) (n = 4). **(I)** Quantification of kidney-resident neutrophils present in *WT* mice under the indicated treatments. *, $P \leq 0.05$ (n = 4). **(J)** Percentage of iT_{REG} cells generated from splenic *WT* and *Vav1*$^{-/-}$ CD4$^+$CD25$^-$ T cells in cell culture (n = 4). **(K)** Extent of kidney fibrosis in AngII-infused *Foxn1*^{nu} mice injected with the indicated iT_{REG} cells as shown in insets. *, $P \leq 0.05$; **, $P \leq 0.01$ relative to either control or indicated experimental pairs (in brackets) (n = 4).

Figure 5
Fabbiano et al.

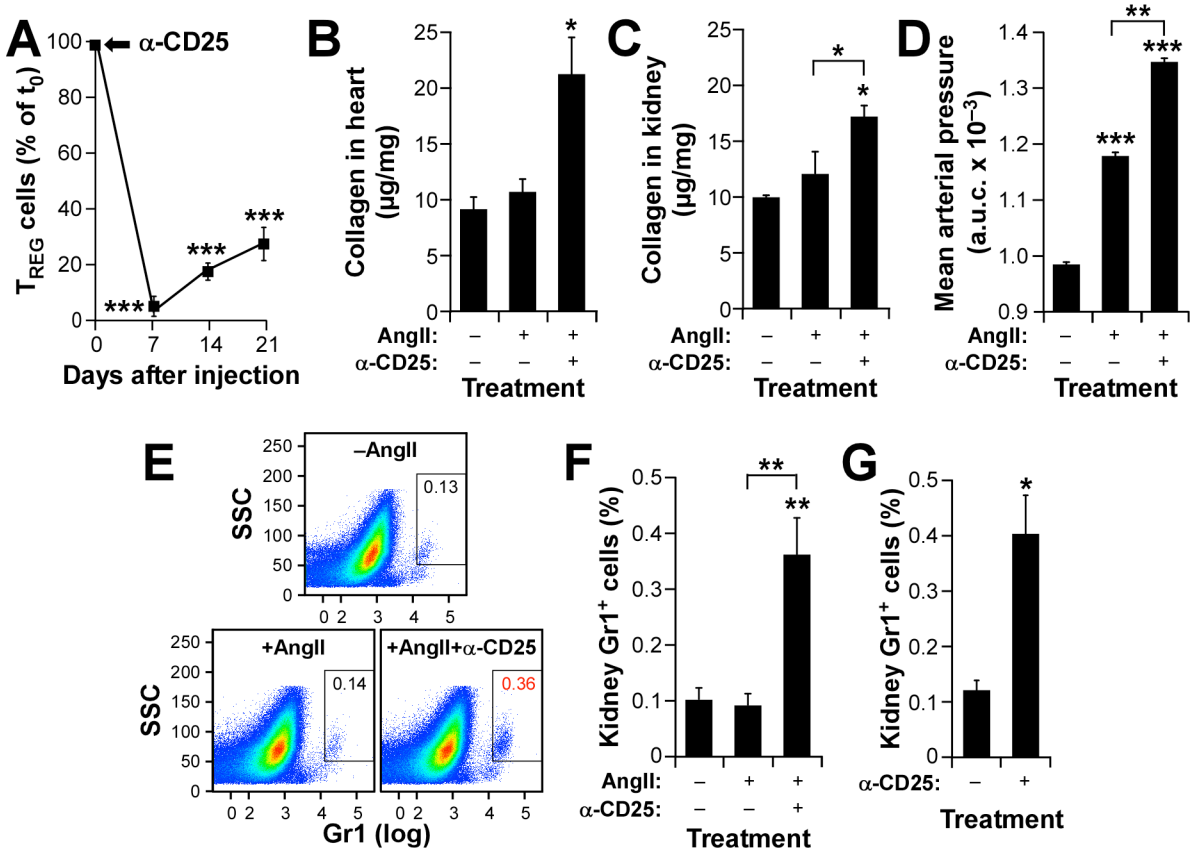

FIGURE 5. The immunodepletion of T_{REG} cells restores renal fibrosis in Vav1-deficient mice. **(A)** Evolution of the $CD4^+CD25^+$ cell population in *Vav1*$^{-/-}$ mice upon immunodepletion with antibodies to CD25. Values are given relative to cell percentages present in the same experimental time point in mice injected with a control antibody. The time of injection (t_0) is indicated with an arrow. ***, $P \leq 0.001$ ($n = 4$). **(B** to **D)** Cardiorenal fibrosis (B and C) and a.u.c. mean arterial pressure levels (D) in *Vav1*$^{-/-}$ mice subjected to indicated experimental conditions. *, $P \leq 0.05$; **, $P \leq 0.01$; ***, $P \leq 0.001$ relative to either control or indicated experimental pairs (in brackets) ($n = 4$). **(E** and **F)** Representative example (E) and quantification (F) of neutrophil numbers present in kidneys

from *Vav1*$^{-/-}$ mice used in above experiments. **, $P \leq 0.01$; relative to either control or indicated experimental pair (in brackets) ($n = 4$). **(G)** Quantification of kidney-resident neutrophils in *Vav1*$^{-/-}$ mice under indicated conditions. *, $P \leq 0.05$ ($n = 4$).

Figure 6
Fabbiano et al.

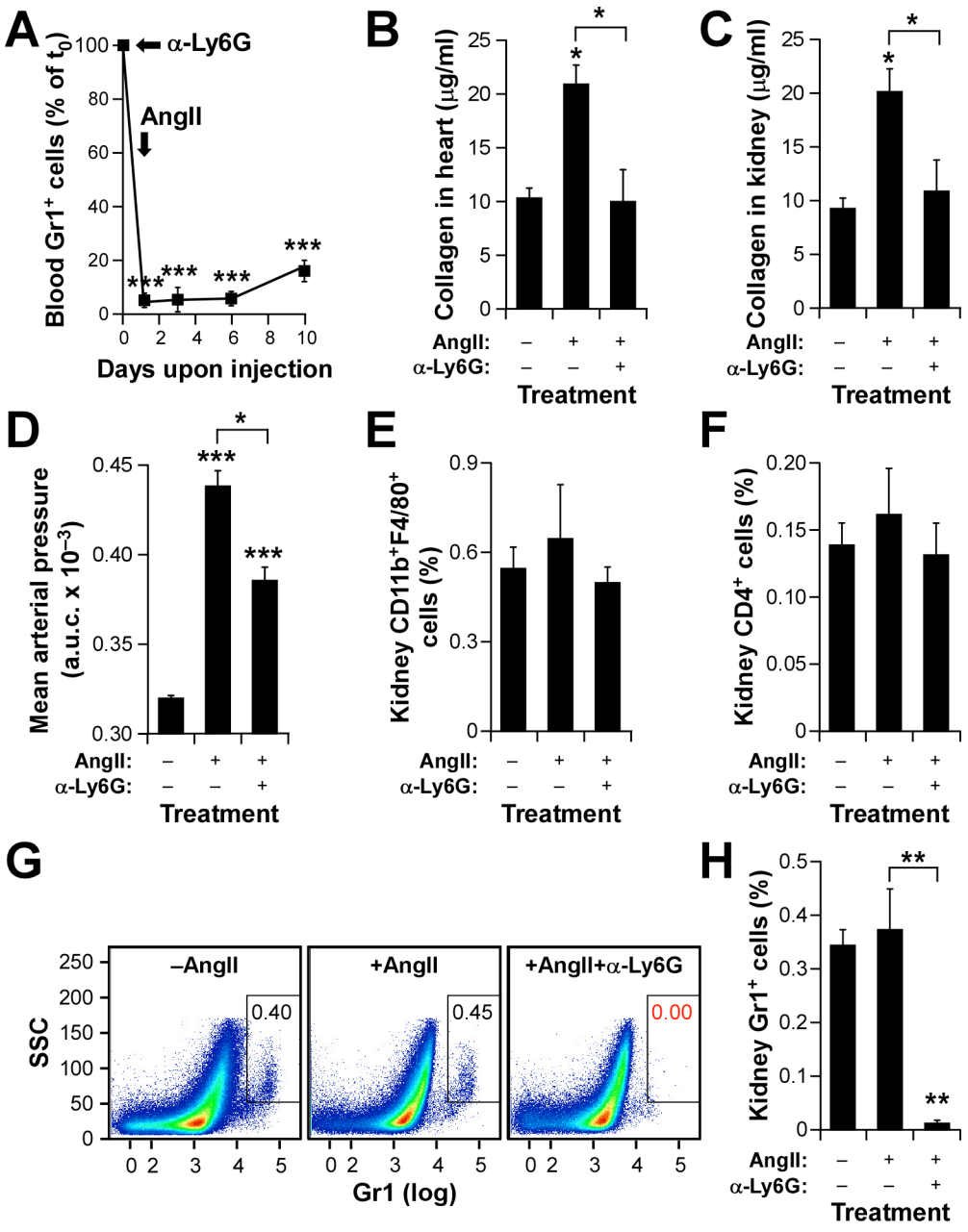

FIGURE 6. Neutrophils are involved in AngII-driven cardiorenal fibrosis. **(A)** Impact of the immunodepletion step in the neutrophil numbers present in *WT* mice. Values are given relative to numbers obtained in mice treated with a control antibody. ***, $P \leq 0.001$ ($n = 4$).

1009 The time points of antibody and implantation of osmotic pumps are indicated by arrows. **(B**
1010 and **C)** Extent of cardiorenal fibrosis obtained in *WT* animals injected with either control or
1011 anti-Ly6G antibodies and, subsequently, infused with AngII as indicated. *, $P \leq 0.05$
1012 relative to either control or indicated experimental pairs (in brackets) ($n = 4$). **(D)** a.u.c.
1013 values of mean arterial pressure increase obtained in the above experiment. *, $P \leq 0.05$;
1014 ***, $P \leq 0.001$ relative to either control or indicated experimental pairs (in brackets) ($n =$
1015 4). **(E** and **F)** Quantification of kidney-resident macrophages (E) and $CD4^+$ T cells (F) at
1016 the end of the above experiments. **(G** and **H)** Representative dot-plots (G) and
1017 quantification (H) of neutrophil numbers present in kidneys at the end of the above
1018 experiments. **, $P \leq 0.01$ relative to either control or indicated experimental pair (in
1019 brackets) ($n = 4$).
1020

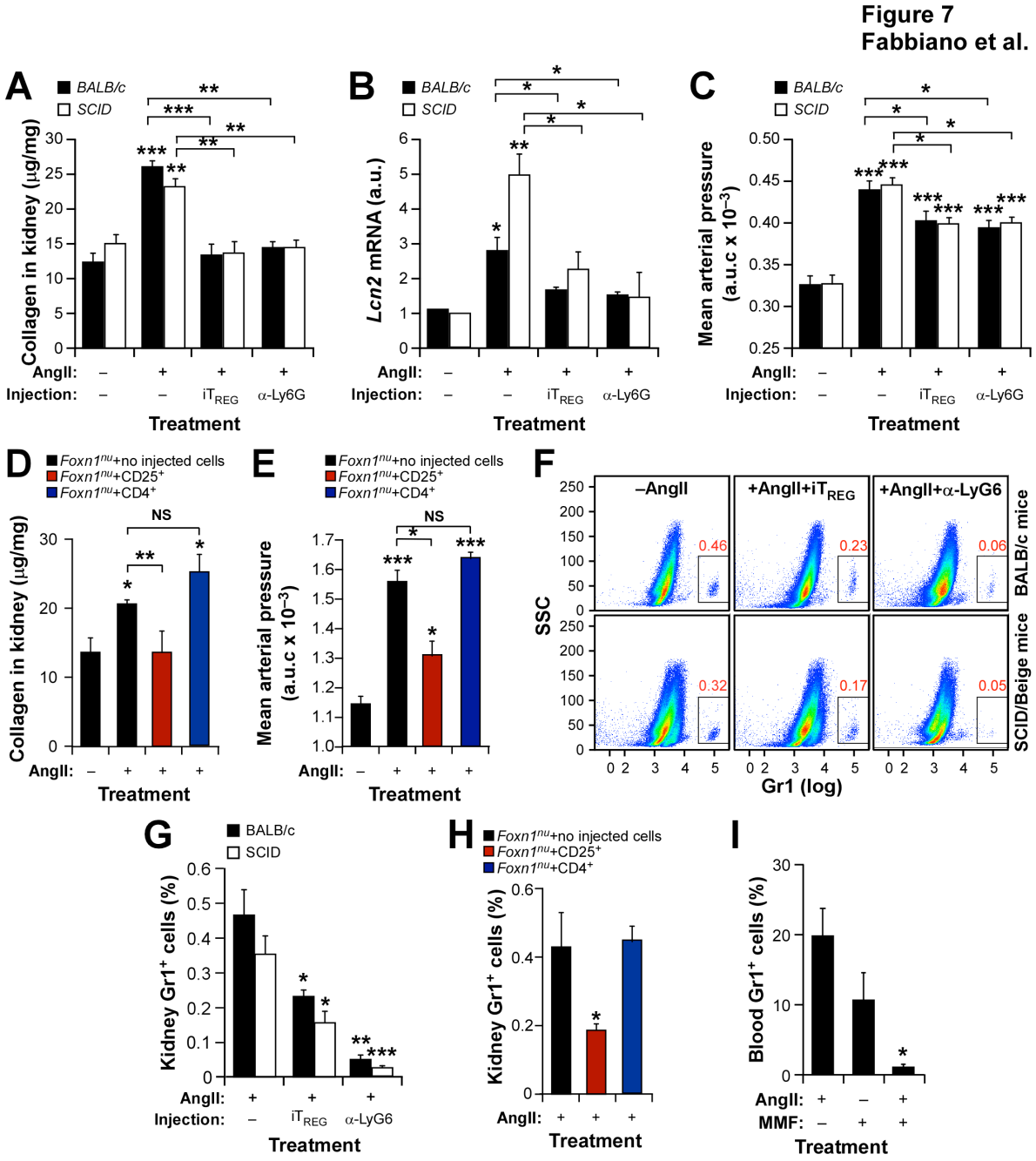

FIGURE 7. T_{REG} cells protect against hypertension-driven fibrosis in an immunosuppression-independent manner. **(A to E)** Renal fibrosis (A and D), kidney abundance of *Lcn2* transcripts (B), and a.u.c mean arterial pressure levels (C and E) in indicated mouse strains and treatment conditions. *, $P \leq 0.05$; **, $P \leq 0.01$; ***, $P \leq 0.001$

relative to either control or indicated experimental pairs (in brackets) (n = 4). **(F** and **G)** Representative dot-plots (F) and quantification (G) of kidney-resident neutrophils in mouse strains and treatment conditions. *, $P \leq 0.05$; **, $P \leq 0.01$; ***, $P \leq 0.001$ relative to either control or indicated experimental pairs (in brackets) (n = 4). **(H** and **I)** Number of kidney-resident and circulating neutrophils present in *Foxn1*^{nu} mice under indicated experimental conditions. *, $P \leq 0.05$ relative to control (n = 4).

Figure 8
Fabbiano et al.

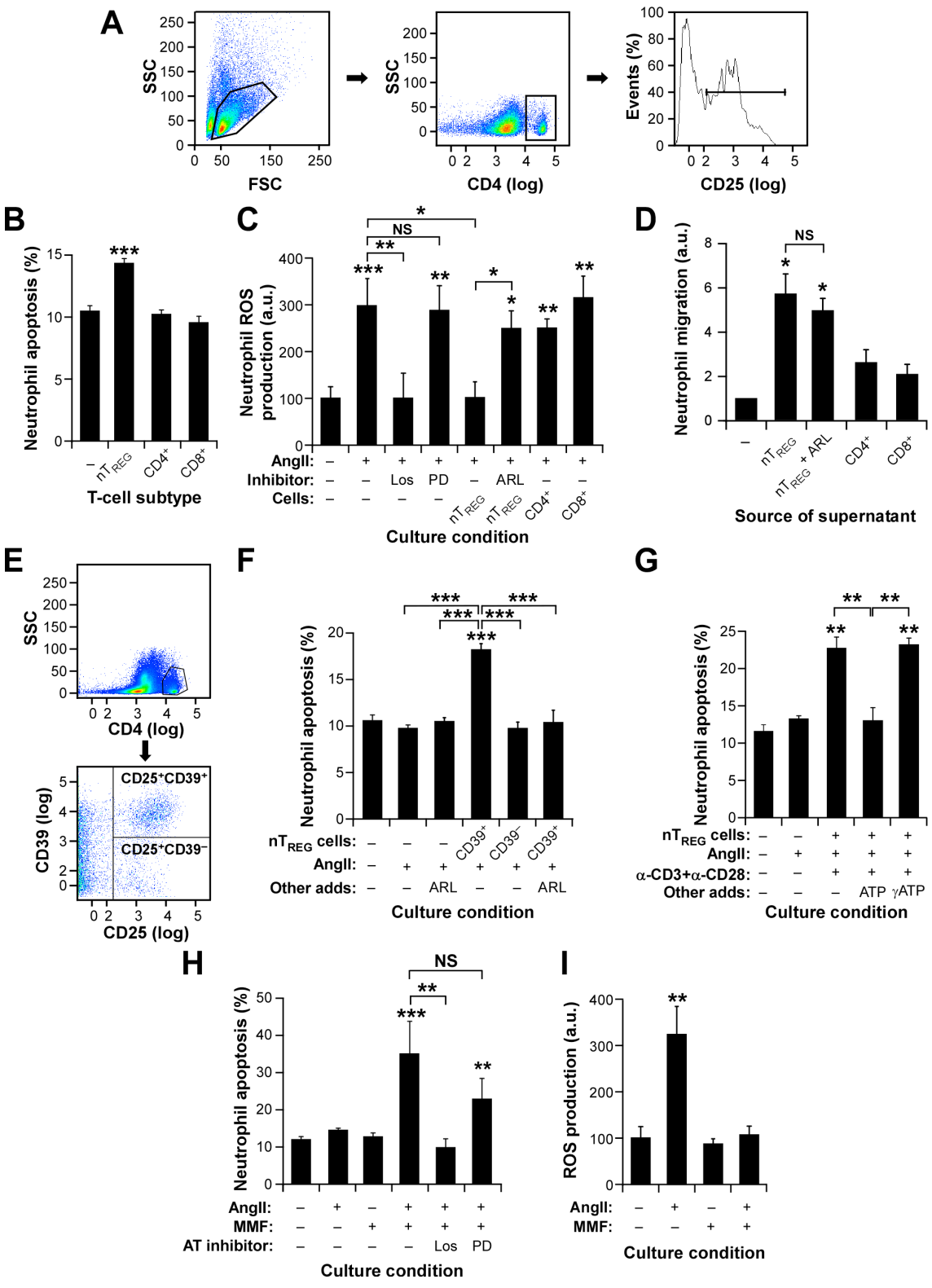

1034

FIGURE 8. T_{REG} cells induce CD39-dependent neutrophil apoptosis. **(A)** Example of the flow cytometry purification step to obtain splenic $CD4^+CD25^+$ nT_{REG} cells used in experiments shown in this figure. **(B** and **C)** Apoptotic response (A) and ROS production (B) of neutrophils under indicated in vitro conditions. ARL, ARL67156; $CD4^+$, $CD4^+CD25^-$ T cells; $CD8^+$, $CD8^+$ T cells; $CD39^+$, $CD4^+CD25^+CD39^+$ nT_{REG} cells; $CD39^-$, $CD4^+CD25^+CD39^-$ nT_{REG} cells; Los, losartan; PD, PD123319. *, $P \leq 0.05$; **, $P \leq 0.01$; ***, $P \leq 0.001$ relative to either control or indicated experimental pairs (in brackets) (n = 4). **(D)** Effect of T_{REG} cell-derived culture supernatants on neutrophil chemotaxis (values obtained with media alone were given an arbitrary value of 1). *, $P \leq 0.05$ relative to control (n = 4). **(E)** Example of the purification step used to obtain splenic $CD39^+$ and $CD39^-$ nT_{REG} cells used in this figure. **(F** to **H)** Apoptotic response of neutrophils under indicated culturing conditions. α-CD3 and α-CD28, antibodies to mouse CD3 and CD28, respectively. **, $P \leq 0.01$; ***, $P \leq 0.001$ relative to either control or indicated experimental pairs (in brackets) (n = 4). **(I)** AngII-stimulated ROS production of neutrophils under indicated culturing conditions. **, $P \leq 0.01$ relative to control (n = 4).

Figure 9
Fabbiano et al.

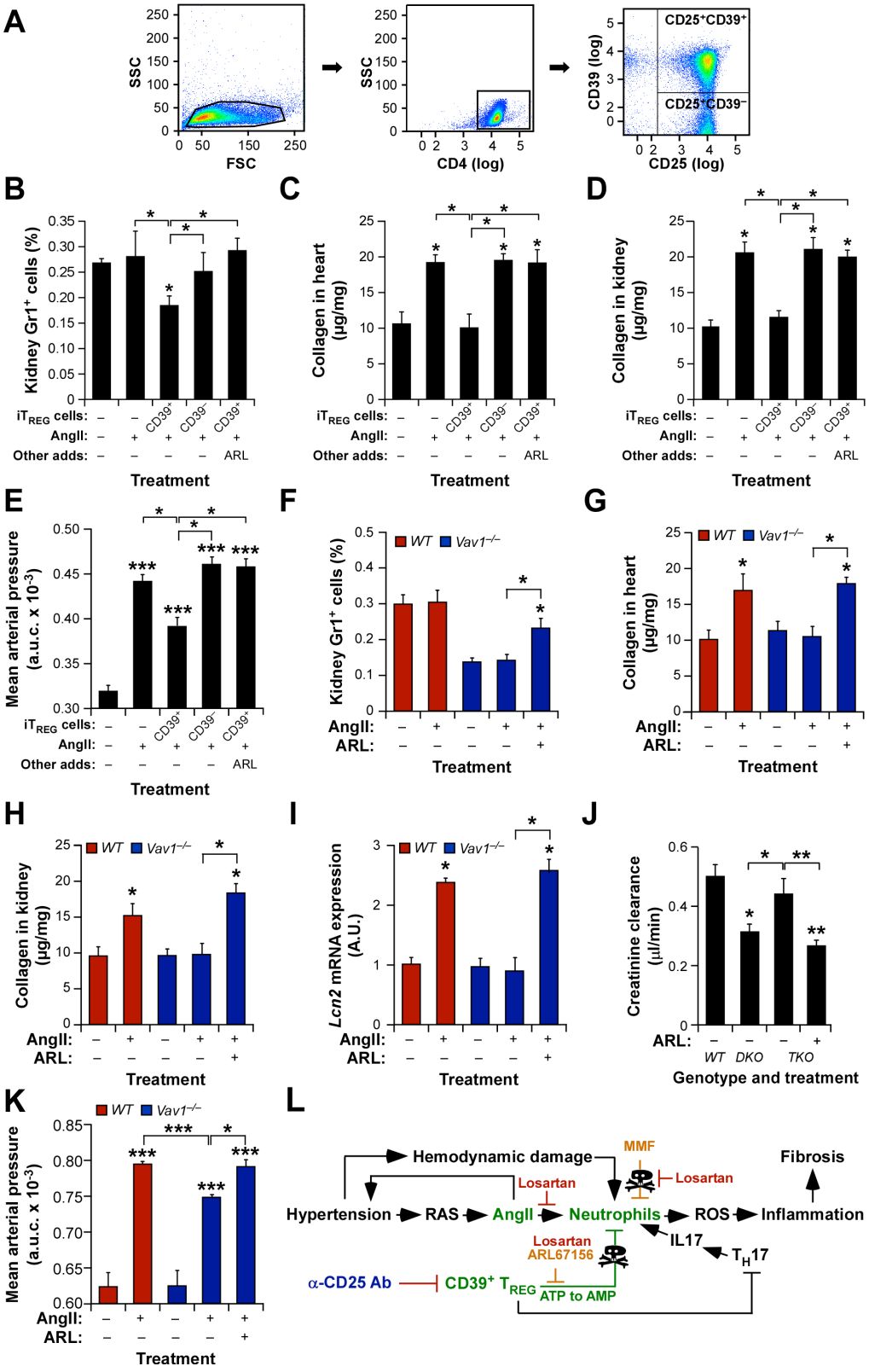

1052

FIGURE 9. $CD39^+$ T_{REG} cells are involved in the protection against AngII-driven cardiorenal dysfunctions. **(A)** Example of the flow cytometry-mediated purification of $CD39^+$ and $CD39^-$ iT_{REG} cells used in these experiments. **(B** to **E)** Percentage of kidney-infiltrating neutrophils (B), extent of cardiorenal fibrosis (C and D), and blood pressure levels (E) in *WT* mice under indicated experimental conditions. *, $P \leq 0.05$; **, $P \leq 0.01$; ***, $P \leq 0.001$ relative to either control or indicated experimental pairs (in brackets) (n = 4). **(F** to **K)** Percentage of kidney-infiltrating neutrophils (F, n = 4), cardiorenal fibrosis (G and H, n = 4), abundance of *Lnc2* transcripts in kidney (I, n = 4), creatinine clearance rates (J, n = 6), and overall blood pressure levels (K, n = 4) in indicated mice and experimental conditions. *, $P \leq 0.05$; **, $P \leq 0.05$; ***, $P \leq 0.001$ relative to either control or indicated experimental pairs (in brackets). **(L)** The new mechanism (green) described in this work. Inhibitors tested exclusively in vitro and in vivo are in red and blue color, respectively. Those used in both conditions are in light brown. The T_{REG}-T_H-neutrophil connection is proposed based on previously published data. RAS, renin-angiotensin system.